

Towards an effective theory of collective oscillations: Neutrino conversion in a neutrino flux

Rasmus S. L. Hansen* and Alexei Yu. Smirnov†

Max-Planck-Institut für Kernphysik,
Saupfercheckweg 1, 69117 Heidelberg, Germany

Abstract

Collective oscillations of supernova neutrinos above the neutrino sphere can be completely described by the propagation of individual neutrinos in external potentials and are in this sense a linear phenomenon. An effective theory of collective oscillations can be developed based on certain assumptions about time dependence of these potentials. General conditions for strong flavor transformations are formulated and these transformations can be interpreted as parametric resonance effects induced by periodic modulations of the potentials. A simplified and solvable example has been studied, where a probe neutrino is propagating in a flux of collinear neutrinos, such that $\nu\nu$ -interactions in the flux are absent. Properties of the parametric resonance are studied, and it is shown that integrations over energies and emission points of the flux neutrinos suppress modulations of the potentials and therefore strong transformations. The transformations are also suppressed by changes in densities of background neutrinos and electrons.

1 Introduction

Neutrino-neutrino scattering results in flavor exchange between the interacting neutrinos [1]. When a given neutrino propagates in the background of

*rasmus@mpi-hd.mpg.de

†smirnov@mpi-hd.mpg.de

other neutrinos, the flavor exchange can be coherent producing both diagonal and off-diagonal potentials. In central regions of supernovae with a large density of neutrinos this coherent flavor exchange may lead to various effects of collective oscillations [2–25].

Finding an exact solution of the evolution equations is an extremely difficult problem and has not been solved in realistic conditions of collapsing stars. With some approximations (stationary situation, symmetries, effective $\nu\nu$ scattering description, elimination of usual matter potential, *etc.*) effects of bi-polar oscillations [2–5], spectral splits/swaps [3, 4, 6–10], and fast flavor transformations in the early evolution [11–18] have been found. In more than one dimension, multi-angle effects (angles of neutrino propagations) can suppress the flavour change [19, 20]. Still strong transitions have been obtained, e.g., in the case of two intersecting fluxes [21, 22].

The main question is whether the flavor transformations that have been found still exist under realistic conditions or they are artefacts of approximations and simplifications. There are some indications that the collective transformations are either very strongly suppressed or lead to flavor equilibration in realistic situations (see e.g. [19, 20, 22–24]). Indeed, strong transitions imply extremely strong correlations between the flavor evolution of neutrinos produced with different energies in different space-time points and at different directions.

In this paper we develop an approach based on the flavour evolution of individual neutrinos rather than the neutrino field. The problem is linear in a sense that will be described in Section 2 and the non-linearity discussed in the literature is a consequence of certain simplifications and approximations which allow the identification of the probe neutrino and background neutrinos. Consequently, the evolution of an individual neutrino can be completely described as propagation in external potentials. These potentials have flavor diagonal as well as flavor off-diagonal terms with non-trivial time (distance) dependence. Using a general parameterisation of the Hamiltonian of evolution we formulate conditions for strong flavor transitions. We show that in the presence of a large matter potential, strong transformations can only be due to a parametric resonance. On this basis one can develop the effective theory of collective oscillations which is based on certain conjectures about the time dependence of the potentials.

In this connection (and as the first step) we consider here a simplified model of the background neutrinos, which still retains the main feature of the coherent flavor exchange. In this model all the background (flux) neutrinos propagate with the same angle, so that $\nu\nu$ interactions in the flux are absent. The latter allows us to explicitly compute the time dependence of the potentials for the probe neutrino. This, in turn, allows to find an explicit

solution to the evolution equation for the probe neutrino. The main feature of the potentials is their periodic (quasi-periodic) dependence on time (distance) which, under certain conditions, leads to the parametric resonance and parametric enhancement of the flavor transition for the probe neutrino.

The simple background model allows us to find an analytic expression for the conversion probability and study the details of the parametric resonance. Furthermore, it allows us to explicitly study the effects of different integrations, in particular, integration over the production point along a given trajectory and averaging over energy. Finally, the effect of a varying matter and neutrino density is explored.

The main question left is to which extent our results for the simplified background can be applied to a realistic case with $\nu\nu$ interactions in the flux.

The paper is organised as follows. In Section 2, after a discussion of the linearity, we construct the Hamiltonian which describes the evolution of individual neutrinos. This allows us to formulate the conditions for strong flavor transformations. In Section 3 we consider a solvable model for the background: Namely the flux of neutrinos propagating with the same angle. We compute the neutrino potentials explicitly and consider approximations for the Hamiltonian which reproduce very well the exact numerical solution. In Section 4 we provide an analytical solution of the problem. In Section 5 we perform integration (averaging) over energies of the flux neutrinos and their production points, while we consider a varying background density in Section 6. Our discussions and conclusions are in Section 7.

2 Towards an effective theory of collective effects

2.1 On linearity

The evolution equation is linear in the sense that a given neutrino does not affect its own flavour evolution. It does not affect the evolution immediately, since the wave function of this neutrino does not appear in the Hamiltonian that describes its flavour evolution. This is related to the fact that $\nu\nu$ interactions are given by the vector product of the corresponding polarisation vectors. Furthermore it does not affect the evolution indirectly: A given neutrino does not affect the evolution of other neutrinos with which it interacts before the interaction point. This is true for SN neutrinos propagating outwards along a straight trajectory without bending.

Linearity in this sense follows from a simple geometric consideration (see Figure 1). The probe neutrino ν_p emitted from the point (\mathbf{x}_0, t_0) interacts

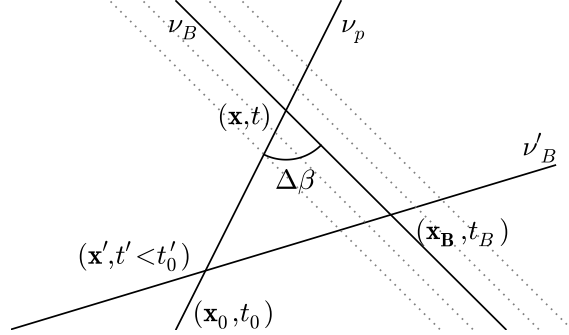


Figure 1: Geometric picture of $\nu\nu$ interactions. t'_0 is the time when ν_p crosses \mathbf{x}' , while t' is the time when another neutrino ν'_p crosses \mathbf{x}' .

in a given space-time point (\mathbf{x}, t) with neutrinos ν_B which move along the trajectory with angle $\Delta\beta$ with respect to the trajectory of ν_p . The previous evolution of ν_B (before collision with ν_p) was not affected by ν_p . The evolution of ν_B can be affected by another background neutrino ν'_B which crosses both the trajectory of ν_B in the point (\mathbf{x}_B, t_B) and the trajectory of ν_p in a point (\mathbf{x}', t') , but it did this before ν_p arrived at \mathbf{x}' , i.e. $t' < t'_0$. The points \mathbf{x}' , \mathbf{x}_B and \mathbf{x} form a triangle: ν_p propagates along the side $\mathbf{x}' - \mathbf{x}$, whereas the background neutrinos should propagate along the two other sides: $\mathbf{x}' - \mathbf{x}_B$ and $\mathbf{x}_B - \mathbf{x}$. The latter trajectory is longer than the former one and therefore the same ν_p can not interact with ν'_B in the point \mathbf{x}'_B and with ν_B in the point \mathbf{x} . Another probe neutrino ν'_p emitted before ν_p can interact with ν'_B in \mathbf{x}' ; then ν'_B interacts with ν_B in \mathbf{x}_B , and in turn, ν_B can interact with ν_p in \mathbf{x} . But ν'_p and ν_p are different neutrinos emitted in different moments of time.

In the stationary situation, ν'_p can be formally identified with ν_p since they have identical flavour evolutions and arrive at \mathbf{x}' in the same flavor state. This is one of the cases where a symmetry leads to effective non-linear equations.

Another effective non-linearity appears when ν'_p , propagating with the same angle as ν_p , is emitted from a space point different from that of ν_p . Then ν'_p can influence the evolution of ν_B and the latter can influence the evolution of ν_p . Again the evolution of ν'_p and ν_p are related since they have the same flavor at the same distance from the production point. This corresponds to a translational symmetry.

Here we have neglected the finite size of the wave packet. If the size of the wave packet is long enough, the first part of the wave packet can in principle influence the last part of the wave packet of a given probe neutrino.

However, this effect has not been considered elsewhere in the literature and will be left for future work.

Due to the absence of non-linearity, we can consider the flavor evolution of individual neutrinos propagating in an external background described by a potential with non-trivial dependence on distance along the trajectory. This description is complete in the sense that all possible effects obtained by solving the equations for neutrino polarisation vectors or density matrices must, if they are real, be reproduced in this description. Inversely, effects which are shown not to exist in our approach should not appear in the usual consideration.

2.2 Evolution equations

We study a probe neutrino with momentum \mathbf{p} which propagates in a medium composed of usual matter including electrons with density n_e and background neutrinos. We consider a 2ν system (ν_e, ν_τ) with vacuum mixing angle θ and mass squared splitting Δm^2 . The eigenfrequency of the probe neutrino is $\omega_p \equiv \Delta m^2/2E$. In numerical computations, we use the value of mixing angle $\theta = 0.1485$ rad ($\sin^2 2\theta = 0.087$), $\omega_p > 0$ for normal mass ordering (NO) and $\omega_p < 0$ for inverted mass ordering (IO). In what follows, we present results for the NO unless IO is explicitly indicated.

The background neutrinos arriving at the space-time point (\mathbf{x}, t) can be characterised by:

1. The flavor at their production; $a = e, \tau$.
2. The 3-momentum \mathbf{k} . Notice that in general, neutrinos are produced with wide energy spectrum which depends on the flavour a .
3. The length of the trajectory l from the production point to the interaction point (\mathbf{x}, t) .

The length l , the momentum \mathbf{k} and (\mathbf{x}, t) determine the production point (\mathbf{x}_0, t_0) . l varies in the interval determined by the width of the neutrino sphere for a given a and momentum \mathbf{k} .

All neutrinos with the same set (a, \mathbf{k}, l) have the same evolution. $n_\nu^a(\mathbf{k}, l)$ denotes the number density of neutrinos emitted from (\mathbf{x}_0, t_0) in the point (\mathbf{x}, t) .

The evolution equation for the flavor of the probe neutrino

$$i\partial_t\psi = H^{(p)}\psi \tag{1}$$

has the Hamiltonian

$$H^{(p)} = \frac{1}{2} \begin{pmatrix} -c_{2\theta}\omega_p + V_e + V_\nu & s_{2\theta}\omega_p + 2\bar{V}_\nu e^{i\phi_B} \\ s_{2\theta}\omega_p + 2\bar{V}_\nu e^{-i\phi_B} & c_{2\theta}\omega_p - V_e - V_\nu \end{pmatrix}, \quad (2)$$

where $V_e \equiv \sqrt{2}G_F n_e$ is the usual matter potential, $c_x \equiv \cos x$, $s_x \equiv \sin x$, while $V_\nu(t)$ and $\bar{V}_\nu(t)e^{i\phi_B(t)}$ ($\bar{V}_\nu > 0$) are the neutrino potentials that describe the neutrino-neutrino interactions.

The diagonal potential V_ν is real and can be written as

$$V_\nu = \sum_a \int d\mathbf{k} \int dl V_\nu^a(\mathbf{k}, l) [\psi_e^a(\mathbf{k}, l) \psi_e^{a*}(\mathbf{k}, l) - \psi_\tau^a(\mathbf{k}, l) \psi_\tau^{a*}(\mathbf{k}, l)], \quad (3)$$

where

$$V_\nu^a(\mathbf{k}, l) \equiv \sqrt{2}G_F n_\nu^a(\mathbf{k}, l) \left[1 - \frac{\mathbf{p} \cdot \mathbf{k}}{|\mathbf{p}| \cdot |\mathbf{k}|} \right].$$

The contribution from scattering of the probe neutrino on antineutrinos $V_{\bar{\nu}}$ can be obtained from the previous expressions for V_ν by the substitutions

$$V_\nu^a \rightarrow -V_{\bar{\nu}}^{\bar{a}}, \quad \psi_x^a \psi_y^{a*} \rightarrow \psi_{\bar{x}}^{\bar{a}*} \psi_{\bar{y}}^{\bar{a}} \quad (4)$$

with $\{x, y\} = \{e, \tau\}$.

We can also introduce the total potential

$$V_\nu^0 \equiv \sum_a \int d\mathbf{k} dl V_\nu^a(\mathbf{k}, l)$$

and the ratio of the potentials

$$\xi \equiv \frac{V_\nu^0}{V_e}, \quad (5)$$

which will play a crucial role in our considerations.

The potential (3) can be rewritten as

$$V_\nu = \int d\mathbf{k} \int dl [V_\nu^e(\mathbf{k}, l)(1 - 2P_{e\tau}(\mathbf{k}, l)) - V_\nu^\tau(\mathbf{k}, l)(1 - 2P_{\tau e}(\mathbf{k}, l))], \quad (6)$$

where $P_{ab}(\mathbf{k}, l) = \psi_b^a(\mathbf{k}, l) \psi_b^{a*}(\mathbf{k}, l)$ is the probability of the transition $\nu_a \rightarrow \nu_b$, and we used the unitarity relation $P_{ae}(\mathbf{k}, l) = \psi_e^a(\mathbf{k}, l) \psi_e^{a*}(\mathbf{k}, l) = 1 - P_{a\tau}(\mathbf{k}, l)$. In the case of T-invariance $P_{\tau e}(\mathbf{k}, l) = P_{e\tau}(\mathbf{k}, l)$, Eq. (6) can be rewritten as

$$V_\nu = \int d\mathbf{k} \int dl [V_\nu^e(\mathbf{k}, l) - V_\nu^\tau(\mathbf{k}, l)](1 - 2P_{e\tau}(\mathbf{k}, l)). \quad (7)$$

The off-diagonal $\nu\nu$ potential in the Hamiltonian (2) equals

$$\bar{V}_\nu e^{i\phi_B} = \sum_a \int d\mathbf{k} \int dl V_\nu^a(\mathbf{k}, l) \psi_e^a(\mathbf{k}, l) \psi_\tau^{a*}(\mathbf{k}, l), \quad (8)$$

and we can obtain the potential for forward scattering on antineutrinos with the substitutions in Eq. (4) as before. Since $\psi_e^a(\mathbf{k}, l) = A_{ae}(\mathbf{k}, l)$, $\psi_\tau^a(\mathbf{k}, l) = A_{a\tau}(\mathbf{k}, l)$, where the latter is the amplitude of probability of the $\nu_a \rightarrow \nu_e$ transition, etc., we can rewrite the integral in (8) as

$$\int d\mathbf{k} \int dl \sum_a V_\nu^a(\mathbf{k}, l) A_{ae}(\mathbf{k}, l) A_{a\tau}^*(\mathbf{k}, l).$$

Then using the unitarity of the evolution matrix (matrix of amplitudes)

$$A_{ee}A_{e\tau}^* + A_{\tau e}A_{\tau\tau}^* = 0,$$

we have

$$\bar{V}_\nu e^{i\phi_B} = \int d\mathbf{k} \int dl (V_\nu^e(\mathbf{k}, l) - V_\nu^\tau(\mathbf{k}, l)) A_{ee}(\mathbf{k}, l) A_{e\tau}^*(\mathbf{k}, l). \quad (9)$$

It can be represented in terms of the oscillation probability as

$$\bar{V}_\nu e^{i\phi_B} = \sum_a \int d\mathbf{k} \int dl (V_\nu^e(\mathbf{k}, l) - V_\nu^\tau(\mathbf{k}, l)) e^{i\phi_B(\mathbf{k}, l)} \sqrt{P_{a\tau}(\mathbf{k}, l)(1 - P_{a\tau}(\mathbf{k}, l))},$$

where

$$\phi_B(\mathbf{k}, l) = \text{Arg}[A_{\tau e}(\mathbf{k}, l) A_{\tau\tau}^*(\mathbf{k}, l)].$$

Then the moduli of the potential, \bar{V}_ν , and the phase ϕ_B equal

$$\bar{V}_\nu = \sqrt{\bar{V}_R^2 + \bar{V}_I^2}, \quad \tan \phi_B = \frac{\bar{V}_I}{\bar{V}_R}, \quad (10)$$

where (suppressing the dependence on (\mathbf{k}, l) except for $\phi_B(\mathbf{k}, l)$)

$$\begin{aligned} \bar{V}_R &= \sum_a \int d\mathbf{k} \int dl (V_\nu^e - V_\nu^\tau) \cos(\phi_B(\mathbf{k}, l)) \sqrt{P_{a\tau}(1 - P_{a\tau})}, \\ \bar{V}_I &= \sum_a \int d\mathbf{k} \int dl (V_\nu^e - V_\nu^\tau) \sin(\phi_B(\mathbf{k}, l)) \sqrt{P_{a\tau}(1 - P_{a\tau})}. \end{aligned}$$

Generalisation to the case of three generations is straightforward. The neutrino potentials disappear if $V_\nu^e(\mathbf{k}, l) = V_\nu^\tau(\mathbf{k}, l)$, and in general, Eq. (7)

and (9) show that the probe neutrino is only affected by the difference $V_\nu^e(\mathbf{k}, l) - V_\nu^\tau(\mathbf{k}, l)$.

The Hamiltonian in Eq. (2) is similar to that for a normal medium, like the Earth, but with non-standard interactions (NSI). The difference from the usual NSI is that we now deal with a strong and non-trivial dependence of these potentials on distance (or time of propagation of the probe neutrino).

Let us remove the complex phases from the Hamiltonian. The off-diagonal element of the Hamiltonian (2) can be rewritten as

$$V' e^{i\phi'},$$

where

$$V' = \sqrt{4\bar{V}_\nu^2 + 4s_{2\theta}\omega_p \cos \phi_B \bar{V}_\nu + s_{2\theta}^2 \omega_p^2}, \quad (11)$$

and the phase ϕ' is determined by

$$\tan \phi' = \frac{2\bar{V}_\nu \sin \phi_B}{2\bar{V}_\nu \cos \phi_B + s_{2\theta}\omega_p} = \frac{\sin \phi_B}{\cos \phi_B + R}. \quad (12)$$

Here

$$R \equiv \frac{s_{2\theta}\omega_p}{2\bar{V}_\nu}$$

is the ratio of the vacuum to the neutrino contributions to the off-diagonal elements of $H^{(p)}$, and \bar{V}_ν is determined by Eq. (10). If the $\nu\nu$ contribution dominates, $\phi' \approx \phi_B$.

The complex phase can be eliminated from the off-diagonal elements, and consequently from the Hamiltonian by performing the transformation

$$\psi = U\psi', \quad U = \text{diag} \left(e^{i\frac{1}{2}\phi'}, e^{-i\frac{1}{2}\phi'} \right). \quad (13)$$

The Hamiltonian of the evolution equation for ψ' is then

$$H^{(p)} = \frac{1}{2} \begin{pmatrix} V^r & V' \\ V' & -V^r \end{pmatrix}, \quad (14)$$

where

$$V^r \equiv V_e + V_\nu - c_{2\theta}\omega_p + \dot{\phi}', \quad (15)$$

and V' is determined in (11). From (12) we find

$$\dot{\phi}' = \frac{(1 + R \cos \phi_B) \dot{\phi}_B + R \sin \phi_B \dot{\bar{V}}_\nu / \bar{V}_\nu}{1 + 2R \cos \phi_B + R^2}.$$

The elimination of the phase from the off-diagonal elements in the Hamiltonian leads to the appearance of $\dot{\phi}'$ in the diagonal elements. It is easy to show that for the neutrino polarisation vector, the transformation (13) goes to a reference frame rotating around the flavor axis z . Therefore, the transformation in Eq. (13) does not change the flavor oscillation probabilities, and the probability for the ψ' state coincide with the probabilities for ψ .

The Hamiltonian in (14) determines the instantaneous mixing angle in the medium θ_m^p for the probe particle via

$$\tan 2\theta_m^p = -\frac{V'}{V^r} = -\frac{\sqrt{4\bar{V}_\nu^2 + 4\omega_p \cos \phi_B s_{2\theta} \bar{V}_\nu + \omega_p^2 s_{2\theta}^2}}{-c_{2\theta}\omega_p + V_e + V_\nu + \dot{\phi}'}, \quad (16)$$

and difference of the eigenvalues

$$\Delta_m^p = \sqrt{V^{r2} + V'^2}.$$

The phase ϕ_B is defined via (8). Here and below we use a super-script p for the probe neutrino and no superscript for the background neutrinos when naming oscillation parameters.

2.3 Conditions for strong flavor transformations

A number of results can be obtained from the general form of the Hamiltonian (14). The key feature is that V^r and V' have an oscillatory dependence on distance (time), which originates from their dependence on the oscillation probabilities $P_{a\tau}(\mathbf{k}, l)$ and the phase ϕ_B . Strong flavor transformations can proceed under the following circumstances:

1. Resonance oscillations. Oscillations with nearly maximal depth occur if

$$V^r \ll V'.$$

Explicitly, the resonance condition reads

$$V_e + V_\nu + \dot{\phi}' - \cos 2\theta\omega_p \approx 0.$$

In the central regions of a star (near the neutrino sphere), $V_e \gg V_\nu \gg c_{2\theta}\omega_p$, so V_e determines the highest frequency in the system. It may happen that

$$\dot{\phi}' \approx -V_e - V_\nu.$$

Under this condition, the system oscillates with nearly maximal depth at a frequency given by V' .

Furthermore, neutrinos and antineutrinos will oscillate in the same way which resembles the regime of bi-polar oscillations [2–5].

2. Adiabatic conversion. Performing a series of field transformations, one can exclude fast time variations in V^r and V' . Then for the rest of the Hamiltonian, the adiabaticity condition may be satisfied and a strong transition occurs if V^r changes from $V^r \gg V'$ to $V^r \ll V'$ (level crossing).
3. Parametric resonance. If $V^r \gg V'$ during the whole evolution, the only possibility for a strong transition is to build up a large transition probability over many periods of oscillations, that is, due to parametric enhancement. The condition for a parametric resonance is that the oscillation period of the probe neutrino T_p coincide with the period of change for the mixing angle T_θ . Since V^r and V' depend on time, the period of oscillations T_p (precession in the polarisation vector picture) is determined from

$$\int_0^{T_p} dt \Delta_m^p = \int_0^{T_p} dt \sqrt{V^{r2} + V'^2} = 2\pi. \quad (17)$$

The mixing angle θ_m^p defined through (16) also has an oscillatory dependence. Denoting the period of this dependence by T_θ , we can write the parametric resonance condition as

$$T_p = T_\theta. \quad (18)$$

Using this general consideration one can develop an effective theory of collective oscillations making various assumptions (conjectures) on the form of potentials which could lead to strong flavor transformations. In what follows we will take the first step in this direction namely consider a simplified situation which allows to find an explicit solution of the evolution equations.

3 Neutrino conversion in a neutrino flux

We illustrate the general results described in Section 2 using a simple model of the background which allows us to explicitly compute the neutrino potentials. This solvable model retains the main feature - the coherent flavor exchange.

We assume that the probe electron neutrino is emitted from the surface at an angle β_p with respect to the surface, and that the frequency of the probe neutrino is ω_p .

3.1 Background model

Let us consider a flux of neutrinos with a wide energy spectrum produced in a layer with width r . We assume that all the flux neutrinos are collinear and

propagate in the same direction. Consequently, there are two key features of the background:

- There is no $\nu\nu$ interactions in the flux since the forward scattering potential is proportional to $(1 - v \cdot v')$.
- There is no feedback of the probe neutrinos onto the flux neutrinos. The effect of a single probe neutrino on the neutrino flux can be neglected. In fact, for a single probe neutrino there is no such interaction even in principle.

Under these conditions, the background neutrinos evolve in the usual way with forward scattering on background electrons which generates a potential V_e .

We consider an original flux of electron neutrinos, while the inclusion of a ν_τ flux can be accounted for by substituting $V_\nu^e \rightarrow (V_\nu^e - V_\nu^\tau)$.

Let us consider first the flux of flux neutrinos with fixed momentum \mathbf{k} and the corresponding frequency

$$\omega_k \equiv \frac{\Delta m^2}{2E_k}.$$

The flux is emitted from the same surface as ν_p at an angle $\pi - \beta_b$.

The evolution equation for the flux neutrino wave function $\psi^T \equiv (\psi_e, \psi_\tau)$ is

$$i\partial\psi = H\psi, \quad (19)$$

where the Hamiltonian has the standard form

$$H = \frac{1}{2} \begin{pmatrix} -c_{2\theta}\omega_k + V_e & s_{2\theta}\omega_k \\ s_{2\theta}\omega_k & c_{2\theta}\omega_k - V_e \end{pmatrix}.$$

It determines the mixing angle in matter θ_m and the level splitting Δ_m for the flux neutrinos:

$$\begin{aligned} \tan 2\theta_m &= \frac{s_{2\theta}\omega_k}{c_{2\theta}\omega_k - V_e}, \\ \Delta_m &= \sqrt{(V_e - c_{2\theta}\omega_k)^2 + s_{2\theta}^2\omega_k^2}. \end{aligned} \quad (20)$$

If the initial state is ν_e , the wave functions of ν_e and ν_τ in the moment of time t equal

$$\begin{aligned} \psi_e(t) &= \cos \frac{1}{2}\Delta_m t + \cos 2\theta_m \sin \frac{1}{2}\Delta_m t, \\ \psi_\tau(t) &= -i \sin 2\theta_m \sin \frac{1}{2}\Delta_m t. \end{aligned} \quad (21)$$

They give the transition amplitudes for $\nu_e \rightarrow \nu_e$ and $\nu_e \rightarrow \nu_\tau$.

Therefore the transition probability $\nu_e \rightarrow \nu_\tau$ is given by

$$P_{e\tau} = |\psi_\tau(t)|^2 = \sin^2 2\theta_m \sin^2 \frac{1}{2} \Delta_m t \approx \left(\frac{\omega_k}{V_e} \right)^2 \sin^2 2\theta \sin^2 \frac{1}{2} \Delta_m t, \quad (22)$$

where in the second equality we used that for $\omega_k \ll V_e$, so that

$$\sin 2\theta_m \approx \frac{\omega_k}{V_e} \sin 2\theta.$$

The probability is strongly suppressed by the electron density. Its maximal value is given by

$$\sin^2 2\theta_m \approx \left(\frac{\omega_k}{V_e} \right)^2 \sin^2 2\theta \approx 10^{-7}, \quad (23)$$

and the period equals $2\pi V_e^{-1} \approx 6 \cdot 10^{-3} \omega_p^{-1}$ for $V_e = 1000 \omega_p$ which we will use as a benchmark value. The depth and length of oscillations are constant.

Using Eq. (21) we find the off-diagonal neutrino potential in Eq. (8):

$$\psi_e \psi_\tau^* = \frac{1}{2} \sin 2\theta_m [-\cos 2\theta_m (1 - \cos \Delta_m t) + i \sin \Delta_m t]. \quad (24)$$

3.2 Evolution of the probe particle. Neutrino potentials

The solution for the flux neutrinos in Eq. (22) and Eq. (24) allows to explicitly compute the neutrino potentials in the equation for the probe particle. The integrals in (3), (6) and (8) are absent, and we have

$$\bar{V}_\nu = V_\nu^0 |\psi_e \psi_\tau^*| = V_\nu^0 \sqrt{P_{e\tau}(1 - P_{e\tau})}, \quad (25)$$

$$\phi_B = \text{Arg}[\psi_e \psi_\tau^*], \quad (26)$$

$$V_\nu = V_\nu^0 (1 - 2P_{e\tau}),$$

and

$$V_\nu^0 = \sqrt{2} G_F n_\nu [1 - \cos(\pi - \beta_p - \beta_b)].$$

$P_{e\tau}$ is given in Eq. (22). For a given moment of time t , the probe neutrino interacts with a flux neutrino which has travelled the distance

$$l = A_\beta t,$$

from the production point, where

$$A_\beta \equiv \frac{\sin \beta_p}{\sin \beta_b}.$$

(We assume $v \approx c$). Therefore, the phase acquired by the flux neutrino when it encounters the probe neutrino equals

$$\phi_m = A_\beta \Delta_m t.$$

This phase should be used in $P_{e\tau}$ and the expressions for the potentials.

For the diagonal potential (15) we have

$$V^r = V_e + V_\nu^0(1 - 2P_{e\tau}) - c_{2\theta}\omega_p + \dot{\phi}'. \quad (27)$$

Using Eqs. (26) and (24) we obtain the phase of the neutrino potentials ϕ_B in terms of phase of the flux neutrinos ϕ_m :

$$\begin{aligned} \cos \phi_B &= \frac{-\cos 2\theta_m(1 - \cos \phi_m)}{\sqrt{\cos^2 2\theta_m(1 - \cos \phi_m)^2 + \sin^2 \phi_m}} \\ &= \frac{-\cos 2\theta_m}{\sqrt{\cos^2 2\theta_m + \cot^2 \frac{1}{2}\phi_m}} \\ &= \frac{-\cos 2\theta_m \left| \sin \frac{1}{2}\phi_m \right|}{\sqrt{1 - P_{e\tau}}}. \end{aligned} \quad (28)$$

Eq. (28) can also be found from the geometric picture in Figure 2.

Notice that for $A_\beta = 1$, the flavor evolution of the probe neutrino and the flux neutrinos are identical. Since flavor exchange in this case does not produce any physical effect, neither flux nor probe neutrinos change (see Appendix A).

The phase of the off-diagonal element of $H^{(p)}$ (12) can be found explicitly in terms of ϕ_m using (28):

$$\tan \phi' = \frac{V_\nu^0 \sin \phi_m}{-V_\nu^0 \cos 2\theta_m(1 - \cos \phi_m) + \Delta_m(\omega_p/\omega_k)}.$$

Then the derivative $\dot{\phi}'$ equals

$$\dot{\phi}' = \Delta_m A_\beta \frac{-\cos 2\theta_m(\cos \phi_m - 1) + \frac{\Delta_m}{V_\nu^0} \frac{\omega_p}{\omega_k} \cos \phi_m}{\left[-\cos 2\theta_m(1 - \cos \phi_m) + \frac{\Delta_m}{V_\nu^0} \frac{\omega_p}{\omega_k} \right]^2 + \sin^2 \phi_m}. \quad (29)$$

The potentials V^r and V' as functions of the neutrino propagation time are shown in Figure 3 for $A_\beta = 1.1001$, and different values of ξ which

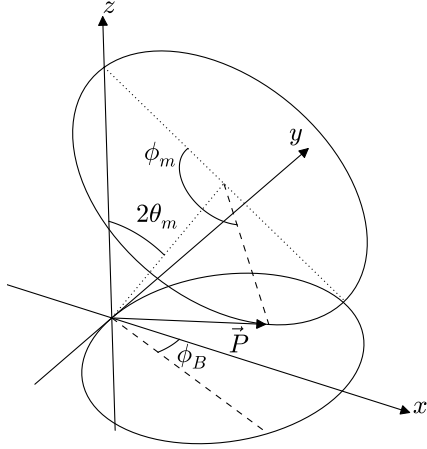


Figure 2: Relationship between ϕ_m , θ_m , and ϕ_B . Eq. (28) is demonstrated in polarisation space. The neutrino polarisation vector is given by $\vec{P} = \psi \vec{\sigma} \psi^\dagger$, where $\vec{\sigma}$ is a 3-vector of Pauli matrices. The upper circle traces out the flavour evolution of ψ , while the lower circle gives the projection of the circle on the xy -plane relevant for ϕ_B .

was defined in Eq. (5). The potentials have periodic dependencies on time. Furthermore, for $\xi = 0.1$, the time dependence can be described by a cosine. For larger ξ there is the deviation from the cosine dependence. Although the sizes of V^r and V' are different, the relative amplitude of the time dependence is of order ξ for both. That will be explained when we derive approximate expressions for V^r and V' .

The exact numerical solution of Eq. (1) with the Hamiltonian from Eq. (14) with V^r given in (27) and (29), and V' in (11) is shown as the red, solid line in Figure 4. We use the same value for V_e as before and for all ξ , A_β is fixed 1% below the value $A_\beta^R = (V_e + V_\nu^0 - \cos 2\theta\omega_p)/\Delta_m$ which we will show is the resonant value in Section 4. According to Figure 4, the interaction with the neutrino flux leads to a moderate (factor of 100) enhancement of the conversion probability for the probe neutrino in the case of $\xi = 0.1$. The period of the fast oscillations is determined by $\Delta_m \approx V_e$, while the long period is given by V_ν . We give a detailed interpretation of these results using an approximate analytical study in Section 4.

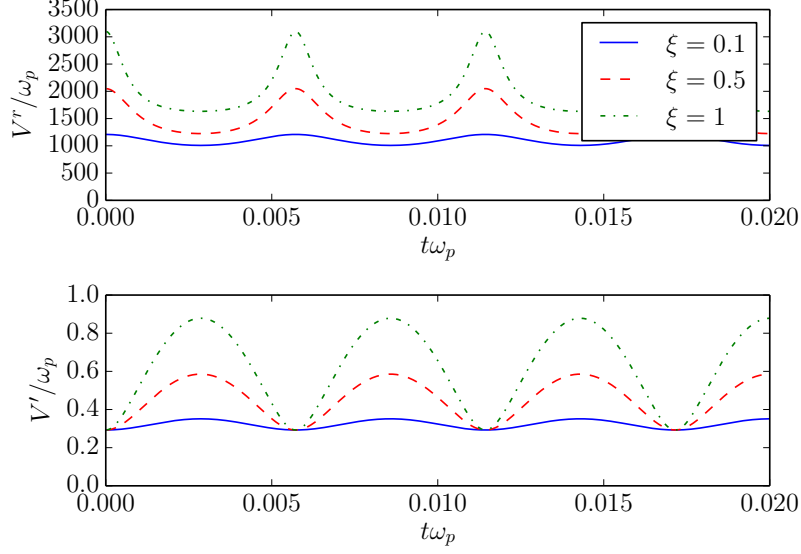


Figure 3: The potentials V^r and V' from Eq. (15) and Eq. (11) as functions of the time. We use $\omega_k = \omega_p$ and $A_\beta = 1.1001$.

3.3 Approximations for the potentials and Hamiltonian

In the following, we present simplified Hamiltonians which reproduce the results of the full calculation to a good approximation and will allow us to find an analytic solution for the oscillation probability of the probe neutrino.

The first approximation is based on the smallness of the oscillation depth of the background neutrino (23). The same quantity gives deviation of $|\cos 2\theta_m|$ from 1. Indeed, according to (23) $P_{e\tau} \leq 10^{-7}$. Therefore we can neglect $P_{e\tau}$ in comparison to 1 and take $\cos 2\theta_m \approx -1$.

In this approximation, \bar{V}_ν (25) can be rewritten using (22) as

$$\bar{V}_\nu \approx V_\nu^0 \sqrt{P_{e\tau}} = s_{2\theta} \xi \omega_k |\sin \tfrac{1}{2} \phi_m|, \quad (30)$$

and from Eq. (28) we obtain

$$\cos \phi_B \approx |\sin \tfrac{1}{2} \phi_m|.$$

The diagonal element of the Hamiltonian (27) becomes

$$V^r \approx V_e \left[1 + \xi - \frac{\omega_p c_{2\theta}}{V_e} + \xi A_\beta \frac{\frac{\omega_p}{\omega_k} \cos \phi_m - \xi(1 - \cos \phi_m)}{\left[\frac{\omega_p}{\omega_k} + \xi(1 - \cos \phi_m) \right]^2 + \xi^2 \sin^2 \phi_m} \right]. \quad (31)$$

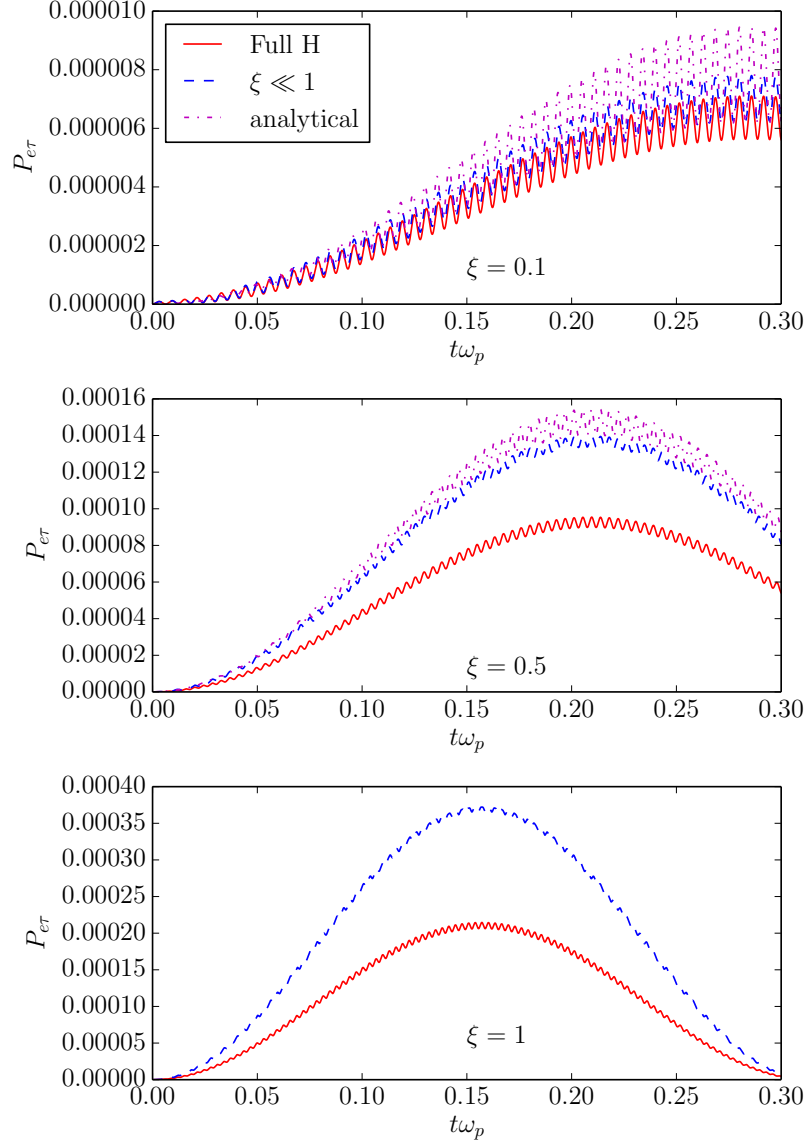


Figure 4: Conversion probabilities as function of time for different ξ close to the parametric resonance. The full solution of Eq. (1) (solid red) uses Eqs. (27) and (11), the approximation (dashed blue) uses Eqs. (33) and (34), while the analytical solution (dash-dotted magenta) is given in Eq. (47). The frequencies are related by $\omega_k = \omega_p$, while $A_\beta = 0.99A_\beta^R$.

The off-diagonal element V' (11) can be written as

$$V' = s_{2\theta}\omega_p \sqrt{1 + 4\xi \frac{\omega_k}{\omega_p} \sin^2 \frac{\phi_m}{2} \left(1 + \xi \frac{\omega_k}{\omega_p}\right)}. \quad (32)$$

We find that the solution of the evolution equation with (32) and (31) practically coincides with the full solution in Figure 4.

Notice that the approximation $P_{e\tau} \ll 1$ may not work if the neutrinos in the background are also subjected to the $\nu\nu$ interaction and their oscillations therefore are parametrically enhanced.

Another simplification can be obtained if the density of neutrinos is much smaller than density of electrons $\xi \ll 1$. In this case we have according to (30)

$$s_{2\theta}\omega_k \gg \bar{V}_\nu,$$

which means that the off-diagonal neutrino potential is suppressed by ξ with respect to the vacuum term. Using Eq. (32), we find

$$V' \approx s_{2\theta}\omega_p \left[1 + 2\xi \frac{\omega_k}{\omega_p} \sin^2 \frac{1}{2}\phi_m\right].$$

It can be rewritten as

$$V' \approx s_{2\theta}\omega_p \left(1 + \xi \frac{\omega_k}{\omega_p} - \frac{\omega_k}{\omega_p} \xi \cos \phi_m\right). \quad (33)$$

For V^r in Eq. (31), we obtain

$$V^r \approx V_e \left(1 + \xi - \frac{c_{2\theta}\omega_p}{V_e} + A_\beta \frac{\omega_k}{\omega_p} \xi \cos \phi_m\right), \quad (34)$$

by neglecting the highest powers of ξ . Let us underline that the periodic term in V^r is mainly due to $\dot{\phi}'$ (after we have neglected $P_{e\tau}$). Periodic contributions to the potentials are due to the $\nu\nu$ scattering and therefore they are proportional to ξ . In every place, $\cos \phi_m$ and ξ enter together in the combination

$$B + \xi \cos \phi_m, \quad B = \mathcal{O}(1).$$

For small ξ the periodic dependence in the potentials can be expanded in series of $\xi \cos \phi_m$, and to lowest order V' and V^r have linear dependencies on $\xi \cos \phi_m$. These linear dependencies are well reproduced by the solid lines in Figure 3 which correspond to $\xi = 0.1$. With an increase of ξ , the approximation breaks down: The lines deviate from the simple dependence on $\cos \phi_m$.

At the same time, the period of oscillations determined by $A_\beta \Delta_m \approx A_\beta V_e$ does not change with ξ . In units of $t\omega_p$, it equals $2\pi 10^{-3}/A_\beta$.

The Hamiltonian with V^r in (34) and V' in (33) can be presented as

$$H^{(p)} = 1/2 \begin{pmatrix} d + h \cos \phi_m & g + f \cos \phi_m \\ g + f \cos \phi_m & -d - h \cos \phi_m \end{pmatrix}, \quad (35)$$

where

$$\begin{aligned} d &\equiv V_e + V_\nu^0 - c_{2\theta}\omega_p, & h &\equiv A_\beta \frac{\omega_k}{\omega_p} V_\nu^0, \\ g &\equiv s_{2\theta}(\omega_p + \xi\omega_k), & f &\equiv -s_{2\theta}\omega_k\xi. \end{aligned} \quad (36)$$

These quantities have the following hierarchy:

$$\begin{aligned} d &\approx V_e, \quad h = \mathcal{O}(\xi V_e), \quad g = \mathcal{O}(s_{2\theta}\omega_p), \quad f = \mathcal{O}(s_{2\theta}\omega_p\xi), \\ d &\gg h \gg g \gg f. \end{aligned}$$

Notice that the off-diagonal elements of $H^{(p)}$ are suppressed with respect to the diagonal ones as

$$\frac{g}{d} \sim \frac{f}{h} \approx \frac{s_{2\theta}\omega_p}{V_e}.$$

Furthermore, in each element of the Hamiltonian, the periodic terms are suppressed by ξ . In the limit $\xi \rightarrow 0$, V^r and V' are reduced to the standard expressions in matter. If higher orders of ξ are included, higher powers of $\cos \phi_m$ appear, and we will obtain a series expansion in $(\xi \cos \phi_m)^k$.

4 Analytic solution of the equation

4.1 Solution for the resonant mode

The Hamiltonian in Eq. (35) is of the type that can give rise to parametric resonances [26–30]. Close to the resonance, the corresponding evolution equation can be solved analytically.

Performing a rotation of the fields $\psi = U'(\theta')\psi'$ by the angle

$$\sin 2\theta' = -\frac{g}{\sqrt{d^2 + g^2}} \approx -\frac{g}{d}, \quad (37)$$

we can diagonalise the constant part of the Hamiltonian (35), so that in the basis ψ' it becomes

$$H' = \frac{\sqrt{d^2 + g^2}}{2} \begin{pmatrix} 1 & 0 \\ 0 & -1 \end{pmatrix} + \frac{1}{2\sqrt{d^2 + g^2}} \cos \phi_m \begin{pmatrix} hd + fg & -hg + fd \\ -hg + fd & -hd - fg \end{pmatrix}.$$

Here we can neglect g^2 in comparison to d^2 and (fg) with respect to (hd) which are of the same order approximations as neglecting $P_{e\tau}$ in comparison to 1. Then the Hamiltonian equals

$$H' \approx \frac{1}{2} \begin{pmatrix} d + h \cos \phi_m & f' \cos \phi_m \\ f' \cos \phi_m & -d - h \cos \phi_m \end{pmatrix}, \quad (38)$$

where

$$f' \equiv f - \frac{gh}{d}. \quad (39)$$

Both terms in f' are of the same order: $f \sim gh/d \sim s_{2\theta\omega_p}\xi$. It can be written as

$$f' = -s_{2\theta\omega_k}\xi \left(1 + \frac{A_\beta(\xi)}{1 + \xi} \right) \approx -2s_{2\theta\omega_k}\xi, \quad (40)$$

where we used $A_\beta = A_\beta^R$ in the second equality.

Next, we will average the periodic dependence in the diagonal elements. Indeed, the effect of the potentials' variation on the oscillation probability is related to variations of the mixing angle. According to the Hamiltonian (38)

$$\tan 2\theta_m^p = \frac{f' \cos \phi_m}{d + h \cos \phi_m} \approx \frac{f'}{d} \left(1 - \frac{h}{d} \cos \phi_m \right) \cos \phi_m.$$

The effect of the periodic term in the diagonal elements given by the second term in the last expression is suppressed by $h/d \sim \xi$. Thus, the variations of the diagonal elements produce small depth modulations of the main mode with higher frequencies.

After averaging over the phase in the diagonal elements, we obtain

$$H' \approx \frac{1}{2} \begin{pmatrix} d & f' \cos \phi_m \\ f' \cos \phi_m & -d \end{pmatrix}.$$

Using $\cos \phi_m = \frac{1}{2}(e^{i\phi_m} + e^{-i\phi_m})$, we can split the Hamiltonian in two parts:

$$H = H_0 + \Delta H,$$

where

$$H_0 = \frac{1}{4} \begin{pmatrix} 2d & f' e^{-i\phi_m} \\ f' e^{i\phi_m} & -2d \end{pmatrix}, \quad (41)$$

and

$$\Delta H = \frac{f'}{4} \begin{pmatrix} 0 & e^{i\phi_m} \\ e^{-i\phi_m} & 0 \end{pmatrix}.$$

(Similarly one can consider another splitting when the phases in H_0 and ΔH switch signs.) This splitting makes sense since only one frequency mode is

enhanced, either $A_\beta \Delta_m$ or $-A_\beta \Delta_m$. If resonance takes place for $A_\beta \Delta_m$, then the part of the Hamiltonian with $-A_\beta \Delta_m$ can be considered as a correction.

Let us make the transformation of the fields

$$\psi' = U_\alpha \psi_\alpha, \quad U_\alpha = \text{diag} \left(e^{-i\frac{1}{2}\phi_m}, \quad e^{i\frac{1}{2}\phi_m} \right)$$

that removes the phases in H_0 (41). Then for the transformed fields ψ_α , the Hamiltonian can be written as

$$H^\alpha = H_0^\alpha + \Delta H^\alpha, \quad (42)$$

where

$$H_0^\alpha = \frac{1}{2} \begin{pmatrix} d - A_\beta \Delta_m & \frac{1}{2} f' \\ \frac{1}{2} f' & -d + A_\beta \Delta_m \end{pmatrix}, \quad (43)$$

(here we included the terms with $A_\beta \Delta_m$ which follow from differentiation of U_α) and

$$\Delta H^\alpha = \frac{f'}{4} \begin{pmatrix} 0 & e^{i2\phi_m} \\ e^{-2i\phi_m} & 0 \end{pmatrix}. \quad (44)$$

Notice that the phase is doubled in ΔH^α .

Let us first find a solution, S_0 , of the evolution equation with the Hamiltonian H_0^α :

$$i\dot{S}_0 = H_0^\alpha S_0, \quad (45)$$

thus neglecting ΔH^α . All the parameters in H_0^α (43) are constants. Therefore the solution to Eq. (45) is the usual oscillation solution with a mixing angle given by

$$\sin 2\theta_m^{\alpha p} = \frac{f'}{2\gamma}, \quad \cos 2\theta_m^{\alpha p} = -\frac{d - A_\beta \Delta_m}{\gamma},$$

where

$$\gamma \equiv \sqrt{(d - A_\beta \Delta_m)^2 + f'^2/4}$$

is the level splitting. The S_0 matrix can be written as

$$S_0 = U_m^p S^{\text{diag}} U_m^{p\dagger}, \quad S^{\text{diag}} = \text{diag}(e^{i\phi_m^p}, \quad e^{-i\phi_m^p}),$$

with the phase

$$\phi_m^p = \frac{1}{2}\gamma t,$$

and U_m^p being a rotation by the angle $\theta_m^{\alpha p}$. Explicitly,

$$S_0 = \cos \phi_m^p \begin{pmatrix} 1 & 0 \\ 0 & 1 \end{pmatrix} + i \sin \phi_m^p \begin{pmatrix} \cos 2\theta_m^{\alpha p} & -\sin 2\theta_m^{\alpha p} \\ -\sin 2\theta_m^{\alpha p} & -\cos 2\theta_m^{\alpha p} \end{pmatrix}. \quad (46)$$

The solution in the flavor basis is then

$$S = U' U_\alpha S_0 U_\alpha^\dagger U'^\dagger.$$

The matrix U' of rotation by the angle θ' (37) can be approximated as

$$U' \approx \begin{pmatrix} 1 & -\frac{g}{2d} \\ \frac{g}{2d} & 1 \end{pmatrix},$$

resulting in

$$S = \cos \phi_m^p I + i \sin \phi_m^p \begin{pmatrix} \cos 2\theta_m^{\alpha p} + \frac{g}{d} \cos \phi_m \sin 2\theta_m^{\alpha p} & -e^{-i\phi_m} \sin 2\theta_m^{\alpha p} + \frac{g}{d} \cos 2\theta_m^{\alpha p} \\ -e^{i\phi_m} \sin 2\theta_m^{\alpha p} + \frac{g}{d} \cos 2\theta_m^{\alpha p} & -(\cos 2\theta_m^{\alpha p} + \frac{g}{d} \cos \phi_m \sin 2\theta_m^{\alpha p}) \end{pmatrix}.$$

Consequently, the transition probability is

$$P_{e\tau}^p = |S_{12}|^2 = \frac{1}{\gamma^2} \left[\frac{f'^2}{4} + \frac{g^2}{d^2} (d - A_\beta \Delta_m)^2 + \frac{g}{d} f' (d - A_\beta \Delta_m) \cos \phi_m \right] \sin^2 \frac{1}{2} \gamma t. \quad (47)$$

The probability averaged over the fast modulations equals

$$P_{e\tau}^p = |S_{12}|^2 = \frac{1}{\gamma^2} \left[\frac{f'^2}{4} + \frac{g^2}{d^2} (d - A_\beta \Delta_m)^2 \right] \sin^2 \frac{1}{2} \gamma t.$$

The expression in Eq. (47) is used for obtaining the dash-dotted magenta curve in Figure 4. So, Eq. (47) provides a good approximation when $\xi \ll 1$, and in order to improve it further, we need to include ΔH^α of Eq. (44) (see Appendix B).

According to Eq. (47), the parametric resonance condition is

$$d = A_\beta \Delta_m. \quad (48)$$

Recall that this condition is obtained after averaging of the diagonal elements of the Hamiltonian in the linear approximation: $d = \langle V_r \rangle$. Under this condition the oscillations in Eq. (47) proceed with maximal depth independently of f' , while the oscillation length is determined by $f'/2$:

$$l_m = \frac{4\pi}{f'} \approx \frac{2\pi}{s_{2\theta} \xi \omega_k} = \frac{1}{s_{2\theta} \xi} l_\nu.$$

Here l_ν is the vacuum oscillation length.

The resonance condition (48) does not depend on t , and modulations are absent. It can be written explicitly as

$$V_e + V_\nu^0 - c_{2\theta} \omega_p = A_\beta (V_e - c_{2\theta} \omega_k).$$

The difference between the left and right hand sides of this equation is the factor A_β and the absence of V_ν^0 on the right hand side. The latter is only the case since in our model, background neutrinos have no $\nu\nu$ interactions. If V_ν^0 would appear on the right hand side, the resonance condition would be reduced to $A_\beta = 1$ for any density and neutrino energy. At this condition, however, the neutrino background effect disappears, as we discussed in sect. 3. For $V_\nu^0 = 0$ it is reduced to the MSW resonance condition $V_e - c_{2\theta}\omega_p = 0$.

With an analytical description of the parametric resonance, the results in Figure 4 can now be analysed. The value

$$A_\beta^R = \frac{d}{\Delta_m} = \frac{V_e(1 + \xi)}{\Delta_m} \approx (1 + \xi), \quad (49)$$

satisfies the resonance condition in Eq. (48). Changing ξ means further departure from the resonance condition which would produce the main effect. Therefore, for the computations in Figure 4, we change A_β simultaneously with ξ in such a way that the departure from resonance remain 1%. That is, A_β increases with ξ according to (49).

Let us introduce the deviation from resonance D

$$D \equiv 1 - A_\beta \frac{\Delta_m}{d},$$

so that

$$d - A_\beta \Delta_m = dD$$

(in our computations $D = 0.01$). From this equation we have

$$A_\beta = (1 - D) \frac{d}{\Delta_m} \approx (1 - D)(1 + \xi)$$

since $\Delta_m \approx V_e$.

For $\xi = 0.1$ there is a good agreement between the results of computations with the exact Hamiltonian and the approximation in Eq. (33) and Eq. (34): The depth and period of the fast modulations are the same. The average value of the probability computed with approximate Hamiltonian is about 10% larger (as expected). With the increase of ξ , the approximation breaks down: for $\xi = 0.5$, and $\xi = 1$ the average probability is 45%, 80% larger correspondingly. So, the deviations approximately increase linearly with ξ .

In terms of D , the frequency of the parametric oscillations squared equals

$$\gamma^2 = d^2 D^2 + \frac{f'^2}{4}, \quad (50)$$

and the depth of parametric oscillations (prefactor in (47)) averaged over fast modulations can be written as

$$P_{e\tau}^{\max} = \frac{f'^2 + 4g^2 D^2}{f'^2 + 4d^2 D^2}. \quad (51)$$

Using expressions for the parameters in Eqs. (39) and (36) and taking for simplicity $\omega_k = \omega_p$, we obtain from (51)

$$P_{e\tau}^{\max} = \frac{\xi^2(1 + A_\beta)^2 + 4D^2(1 + \xi)^2}{\xi^2(1 + A_\beta)^2 + 4(V_e/s_{2\theta}\omega_p)^2 D^2(1 + \xi)^2}. \quad (52)$$

The second term in the nominator and the first term in the denominator can be neglected, so that

$$P_{e\tau}^{\max} \approx \frac{s_{2\theta}^2 \omega_p^2 \xi^2 [2 - D + (1 - D)\xi]^2}{4D^2 V_e^2 (1 + \xi)^2}. \quad (53)$$

For selected values of parameters, we have

$$P_{e\tau}^{\max} \approx 2.2 \times 10^{-4} \frac{\xi^2(2.01 + \xi)^2}{(1 + \xi)^2}.$$

Thus, the depth increases with ξ (almost as ξ^2 for small ξ).

In the expression for the frequency (50), the first term dominates

$$\gamma \approx dD = DV_e(1 + \xi). \quad (54)$$

Correspondingly, the period of parametric oscillations

$$T = \frac{2\pi}{\gamma} = \frac{2\pi}{1 + \xi} \frac{1}{DV_e}$$

decreases with the increase of ξ for fixed D .

For the results of the approximate computations (blue, dashed lines) there is a perfect agreement with the results of the formulas for the depth (53) and frequency (54). These approximations are in a good agreement with the exact computations for $\xi = 0.1$. However, for larger $\xi = 0.5$ and $\xi = 1.0$, the approximate results differ substantially from the exact result.

The relative depth of the high frequency modulations is given by

$$\frac{4g}{d} \frac{d - A_\beta \Delta_m}{f'} \approx 4D \frac{1 + \xi}{\xi(2 + \xi)}$$

according to (47), and it decreases with the increase of ξ . These fast modulations have a larger depth in the approximate analytic expression than in

the exact solution. The non-resonance contribution to the Hamiltonian due to ΔH also leads to high frequency modulations, and the two contributions can cancel each other. Notice that this cancellation can not be inferred immediately from the results in Appendix B which are only valid exactly in the resonance. In resonance, the modulations of the approximate probability (47) disappear.

4.2 The parametric resonance

Let us study the parametric resonance in more details. In Figure 5 the full solution and the approximate solutions are shown together at resonance and for values of ω_k/ω_p close to resonance. The depth of oscillations and the period satisfy the standard relation: $P_{e\tau}^{\max}/l_m^2 \approx \text{constant}$.

In general, the resonance condition can be formulated using physical variables: The period of rotation of the neutrino polarisation vector T_p , and the period of change of mixing angle (which determines the axis of precession), T_θ . The former is determined by the condition in Eq. (17), and the latter (the period of the axis motion) is given by

$$T_\theta = \frac{2\pi}{A_\beta \Delta_m}$$

in our example. Therefore the exact resonance condition (18) becomes

$$A_\beta \Delta_m = \sqrt{V^r{}^2 + V^2} \approx V^r,$$

assuming that $V_e \gg V_\nu^0, \omega_p$, which coincides with Eq. (48).

The dependence of the parametric oscillation depth on ω_k has a resonance character. In Figure 6 we show $P_{e\tau}^{\max}$ as a function of ω_k/ω_p for all other parameters being fixed in such a way that the resonance satisfied is at $\omega_k/\omega_p = 1$.

Let us consider the depth of parametric oscillations averaged over fast modulations. Then the shape of the resonance can be obtained from our analytical results in Eq. (53). In resonance, $D = 0$, the second term in both nominator and denominator of (52) vanish, and the conversion probability equals 1. Close to resonance, the second term in the nominator of Eq. (53) is suppressed with respect to the first term by $(\omega_p/V_e)^2$ and can be safely neglected. Consequently, the depth of oscillations can be written as

$$P_{e\tau}^{\max} = \left[1 + 4 \frac{d^2}{f'^2} \left(1 - A_\beta \frac{\Delta_m}{d} \right)^2 \right]^{-1}. \quad (55)$$

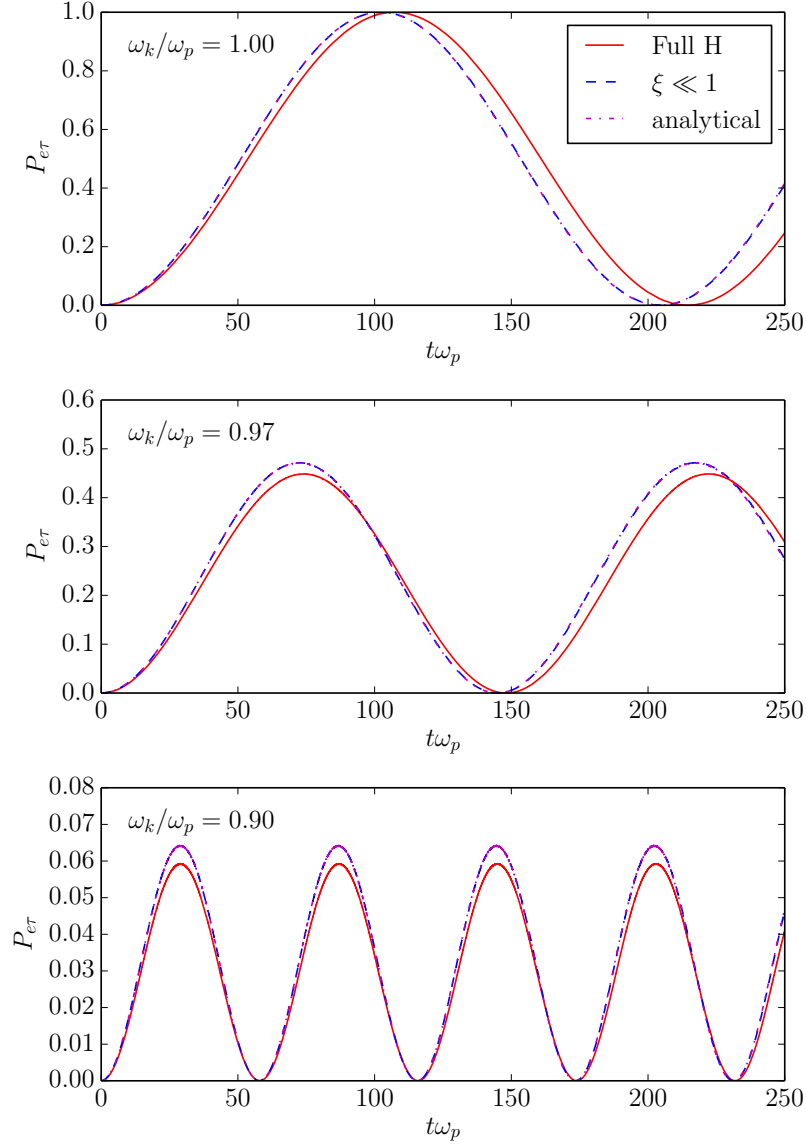


Figure 5: Parametric oscillations: The dependence of the probability $P_{e\tau}$ on time of evolution for different values of ω_k/ω_p . The upper panel is at resonance, while the middle and lower panels are detuned as indicated. The other parameters are $\xi = 0.1$, and $A_\beta = 1.1001$. The lines are calculated using the same equations as in Figure 4.

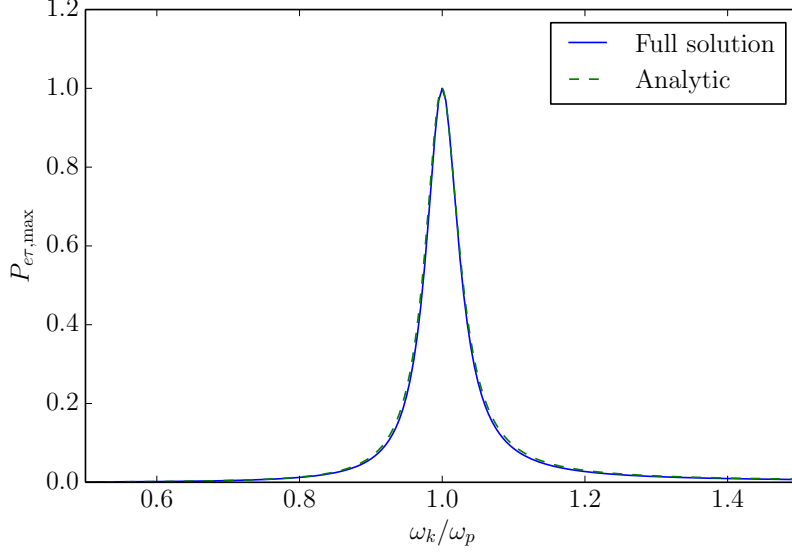


Figure 6: Parametric resonance: Dependence of the depth of parametric oscillations on frequency of the background neutrinos for the exact numerical solution (solid line) and the analytic solution (dashed line). We use $V_\nu^0 = 100\omega_p$ and $A_\beta = 1.1001$.

According to this expression, the resonance width at half the height (the expression above equals 1/2) is determined by the condition

$$2 \frac{d}{f'} \left| 1 - A_\beta \frac{\Delta_m}{d} \right| = 1. \quad (56)$$

The resonance value of Δ_m equals

$$\Delta_m^R = \frac{d}{A_\beta},$$

and in turn, Δ_m^R determines the resonant frequency ω_k^R . In terms of Δ_m^R we have

$$D = 1 - A_\beta \frac{\Delta_m}{d} = 1 - \frac{\Delta_m}{\Delta_m^R}. \quad (57)$$

Using the approximate expression

$$\Delta_m \approx V_e \left(1 - c_{2\theta} \frac{\omega_k}{V_e} \right),$$

we obtain from Eq. (57)

$$1 - \frac{\Delta_m}{\Delta_m^R} = c_{2\theta} \frac{\omega_k - \omega_k^R}{V_e}. \quad (58)$$

Insertion of (58) in (56) gives

$$2 \frac{d}{f'} c_{2\theta} \frac{|\omega_k - \omega_k^R|}{V_e} = 1.$$

Using the expressions for d and f' in the lowest order in ξ , we obtain

$$|\omega_k - \omega_k^R| \approx \frac{1}{2} f',$$

i.e., the width is determined by the off-diagonal element of the Hamiltonian. The relative width of the resonance defined as

$$\frac{\Gamma_\omega}{\omega_k^R} \equiv 2 \frac{|\omega_k - \omega_k^R|}{\omega_k^R} = s_{2\theta} \xi (1 + A_\beta). \quad (59)$$

For the values of parameters we use, this gives $\Gamma_\omega/\omega_k^R = 0.065$ in very good agreement with the result of Figure 6. The width increases with ξ , so that for large ξ one expects strong transformations in a wider energy range.

4.3 Inverted mass ordering and a probe antineutrino

A change of mass ordering from the normal to inverted one means $\omega \rightarrow -\omega$. For the normal ordering, the difference of the eigenstates is $H_{2m} - H_{1m} = \Delta_m (|\omega|)$, where $\Delta_m > 0$ is defined in (20)¹. Therefore $\phi_m = (H_{2m} - H_{1m})t = \Delta_m t$, $\cos 2\theta_m = (\cos 2\theta\omega - V_e)/\Delta_m$, and $\sin 2\theta_m = \sin 2\theta\omega/\Delta_m$. For $V_e \gg \omega$, the mixing parameters are $\cos 2\theta_m \approx -1$ and $\sin 2\theta_m \approx 0$ ($\sin 2\theta_m > 0$). In the case of inverted ordering, $H_{2m} - H_{1m} = -\Delta_m (-|\omega|)$, so that $\phi_m = -A_\beta \Delta_m t$. Now $\cos 2\theta_m = (\cos 2\theta|\omega| + V_e)/\Delta_m$, and $\sin 2\theta_m = \sin 2\theta|\omega|/\Delta_m$. Consequently, the resonance condition for the inverted ordering is satisfied for $e^{i\phi_m}$ and not $e^{-i\phi_m}$ in the decomposition of $\cos \phi_m$ in Eq. (41).

Let us consider a probe antineutrino. The corresponding Hamiltonian, \bar{H} , can be obtained from Eq. (2) by taking the complex conjugate of the phase factors and changing the sign in front of V_e , V_ν^0 , and \bar{V}_ν . Consequently, the resonance condition becomes $A_\beta \Delta_m = -d$. To satisfy this equality, the opposite sign of ϕ_m must be chosen in H_0 in Eq. (41), like in the case of IO. The transition probability for a probe antineutrino is very similar to the transition probability for a probe neutrino for the simple model that has been considered here. Therefore, the analytical approximation in Eq. (47) is also valid for $\bar{\nu}$ as a probe particle if $d = -V_e - V_\nu^0 + c_{2\theta}$, $f = s_{2\theta}\omega_k\xi$, and

¹Recall that the levels are enumerated by according to the flavor content in vacuum.

$g = s_{2\theta}(\omega_p - \xi\omega_k)$ are used, and $(d - A_\beta\Delta_m)$ is replaced by $(d + A_\beta\Delta_m)$. This means that in the same background, a probe ν and a probe $\bar{\nu}$ will evolve in almost the same way. They will both have a parametric resonance and almost the same transition probabilities. This can potentially reproduce the bipolar oscillations.

5 Integrations

The results obtained in Sections 3 and 4 correspond to a neutrino flux with fixed energy, angle and production point. Let us perform the integration of potentials over energies and production points (see general formulas (3) and (8)). This integration does not change the dynamics of propagation. In the present model, the strong transitions stem entirely from the periodicity of the neutrino background flavor, and therefore the integration which leads to averaging of phases will suppress the flavor transformations.

5.1 Integration over production point

Integration over the production point is due to the finite width of the neutrino sphere. Notice that usually the width of the neutrino sphere is ignored when discussing collective oscillations in supernovae, although the effects that can arise due to different neutrino spheres for ν_e , $\bar{\nu}_e$ and ν_x have recently been considered (see e.g. [11–14, 31]). The reason for ignoring the width is that the large density of electrons keeps the neutrino flavor frozen well beyond the neutrino sphere.

The Hamiltonian in Eq. (35) depends on the production point through the phase ϕ_m and the distribution of neutrino sources, $n_\nu(l)$. Of these two, the dependence on ϕ_m is most important since strong flavor conversion mainly arises from a parametric resonance where the frequency $\dot{\phi}_m$ is in resonance with the oscillation frequency of the probe neutrino. If sources of neutrinos are distributed in the interval r with density dn_ν/dl , averaging of oscillatory terms is given by the integral

$$\langle n_\nu \cos \phi_m \rangle = \int_{l-r}^l dl' \frac{dn_\nu(l')}{dl'} \cos(\Delta_m A_\beta l'). \quad (60)$$

If the neutrino sources are uniformly distributed in r , so that $dn_\nu/dl = n_\nu/r$,

the integral in Eq. (60) can be computed:

$$\begin{aligned}\langle n_\nu \cos \phi_m \rangle &= \frac{n_\nu}{r} \int_{l-r}^l dl' \cos \Delta_m A_\beta l' \\ &= \frac{n_\nu}{r} \frac{1}{\Delta_m A_\beta} [\sin \Delta_m A_\beta l - \sin \Delta_m A_\beta (l-r)].\end{aligned}\quad (61)$$

This shows that the oscillatory term is suppressed by a factor

$$2 \frac{1}{r \Delta_m A_\beta} \approx \frac{1}{V_e A_\beta r}. \quad (62)$$

A typical neutrino sphere has a radius ~ 10 km, and for a simple model of the density and temperature profile during the accretion phase [32], the width can be estimated to be $\sim 10\%$ or ~ 1 km. On the other hand, for densities close to the neutrino sphere

$$\frac{1}{\Delta_m A_\beta} \approx \frac{1}{V_e A_\beta} \sim (10^{-3} - 10^{-2}) \text{ cm}.$$

Therefore the suppression factor (62) equals $\sim (10^{-8} - 10^{-6})$, which means that the integration washes out the oscillatory terms of the Hamiltonian. Actually, the parametric resonance is not removed by the integration in Eq. (61), but the conversion scale increases by at least a factor of 10^6 . Without the suppression the conversion scale equals $\gamma \sim 10^{-2} \text{ km}^{-1}$. With the suppression, the conversion scale becomes $\sim 10^4 \text{ km}$. i.e., it extends far beyond the dense part of a supernova.

If the periodic terms vanish, the rest of the Hamiltonian in (35), given by d and g , coincides with the standard Hamiltonian in matter. The only difference is a small constant correction due to V_ν^0 . This leads to oscillations with very small depth suppressed by $s_{2\theta}\omega_p/(V_e + V_\nu)$.

5.2 Integration over neutrino energy

The integration over energy (frequency) produces a smaller suppression effect since the energy enters Δ_m which is relevant for the phase averaging with a suppression. Indeed, expanding the phase we have

$$\phi_m \approx \phi_k = (V_e - c_{2\theta}\omega_k)t, \quad (63)$$

and the second term in brackets is three orders of magnitude smaller than the first one for the parameters that we consider. The effect of integration over ω on the time dependence of $P_{e\tau}$ is shown in Figure 7. For fixed $\omega_k/\omega_p = 1$,

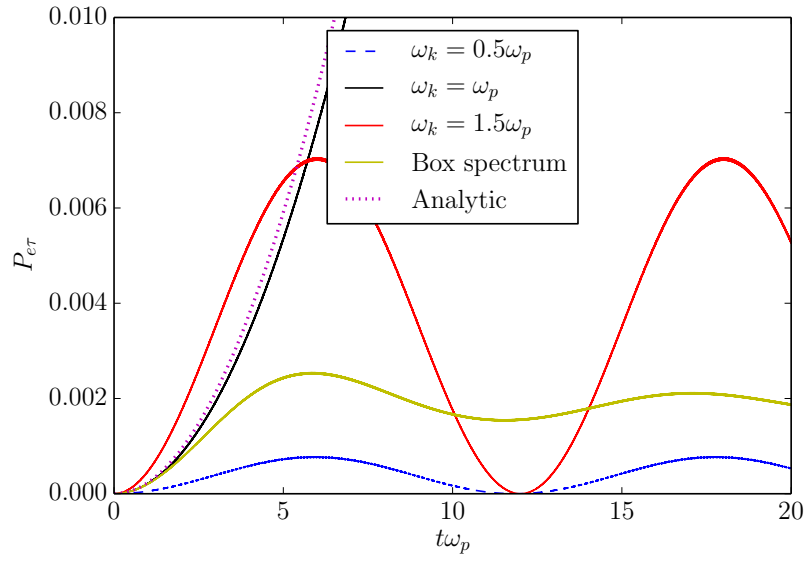


Figure 7: The effect of integration over the energy spectrum on $P_{e\tau}$ as function of evolution time. The conversion probability $P_{e\tau}$ is shown for different energies, ω_k . The frequency $\omega_k = \omega_p$ corresponds to resonance, so that $P_{e\tau}$ eventually reaches 1, while $\omega_k = 0.5\omega_p$ and $1.5\omega_p$ are off resonance. The box-like neutrino spectrum extends from $0.5\omega_p$ to $1.5\omega_p$. The analytic approximation for $\omega_k = \omega_p$ from Eq. (47) is also shown. The other parameters we use are $V_\nu^0 = 100\omega_p$ and $A_\beta = 1.1001$.

the maximal $P_{e\tau}$ is 1, while it is reduced down to 2×10^{-3} for the box-type spectrum.

To understand the effect let us consider the averaging of the off-diagonal element in the Hamiltonian (35) in the interval $(\omega_k - \Delta\omega) - (\omega_k + \Delta\omega)$:

$$\langle \frac{1}{2} f \cos \phi_m \rangle = \frac{s_{2\theta} \xi}{4\Delta\omega} \int_{\omega_k - \Delta\omega}^{\omega_k + \Delta\omega} d\omega'_k \omega'_k \cos \phi_k(\omega'_k), \quad (64)$$

where ϕ_k is defined in Eq. (63). The integration in (64) gives

$$\langle \frac{1}{2} f \cos \phi_m \rangle = \frac{s_{2\theta} \xi}{2\Delta\omega (c_{2\theta} t)^2} [c_{2\theta} t \omega_k \sin \Delta\phi \cos \phi_k + (\sin \Delta\phi - \Delta\phi \cos \Delta\phi) \sin \phi_k], \quad (65)$$

where $\Delta\phi \equiv c_{2\theta} t \Delta\omega$ is the difference of phases due to the difference of frequencies.

The integration over frequency (energy) leads to additional time dependence of the oscillatory terms. At the condition $\Delta\phi \ll 1$ (early times), which can be written as

$$t \ll t_c \equiv \frac{1}{c_{2\theta} \Delta\omega}, \quad (66)$$

the expression (65) is reduced to the original one: $\frac{1}{2} s_{2\theta} \xi \cos \phi_k$ with a single central frequency.

For later times, $t > t_c$, the oscillatory terms are suppressed as

$$\langle \frac{1}{2} f \cos \phi_m \rangle = \frac{1}{2} s_{2\theta} \xi \omega_k \cos \phi_k \frac{\sin \Delta\phi}{c_{2\theta} \Delta\omega t}.$$

Thus, the transition probability is parametrically enhanced at $t < t_c$ in the way we discussed above, whereas at $t > t_c$ enhancement is terminated due to suppression of the oscillatory terms, and the probability converges to a constant.

One can estimate this asymptotic probability in the following way. According to (47) the transition probability in the moment of time t_c at the resonance frequency, ω_k^R , equals:

$$P_{e\tau}^p = \sin^2 \frac{1}{2} \gamma(\omega_k^R) t_c \approx \left[\frac{1}{2} \gamma(\omega_k^R) t_c \right]^2 \approx \left[\frac{s_{2\theta} \xi \omega_k^R}{2c_{2\theta} \Delta\omega} \right]^2, \quad (67)$$

where we used that at resonance $\gamma \approx f'/2 \approx 2s_{2\theta} \xi \omega_k^R$. The probability increases with ξ and with the decrease of the integration interval $\Delta\omega$.

Integration over energy also leads to a shift of the effective resonance frequency to larger values due to the presence of ω'_k under the integral in

(64). In our computations $\omega_k^R/\Delta\omega \sim 2$. Therefore, the probability in Eq. (67) becomes

$$P_{e\tau}^p = \left[\frac{s_{2\theta}\xi}{2c_{2\theta}} \right]^2 \sim 10^{-3}$$

in good agreement with the upper panel in Figure 7. This consideration means that one should consider another regime when ξ is not small: $\xi \geq 1$ in order to have strong transitions in the present model.

Notice that the integration over energy is equivalent to the effect of loss of coherence due to the spatial separation of neutrino eigenstates wave packets. Indeed, complete separation occurs during the time

$$t_{\text{coh}} = \frac{l_\nu}{2\pi} \frac{E}{\Delta E}.$$

On the other hand using

$$\Delta\omega = \frac{\Delta m^2}{2E^2} \Delta E = \frac{2\pi}{l_\nu} \frac{\Delta E}{E},$$

we find from (66) that $t_c = t_{\text{coh}}$.

6 Varying densities

6.1 Adiabaticity and asymptotic values of $P_{e\tau}$

Let us first consider the change of the density of electrons $V_e(r)$ on the neutrino oscillations. The typical scale of density change in a SN r_d is much larger than the oscillation length:

$$r_d = V_e \left(\frac{dV_e}{dr} \right)^{-1} \sim r \gg \frac{1}{V_e}.$$

Therefore the change of density is adiabatic, and we can use the adiabatic approximation result for $P_{e\tau}$ in the formulas of the previous sections:

$$P_{e\tau} = \frac{1}{2} [1 - \cos 2\theta_m(t_0) \cos 2\theta_m(t) - \sin 2\theta_m(t_0) \sin 2\theta_m(t) \cos \phi_m],$$

where $\theta_m(t_0)$ and $\theta_m(t)$ are the values of the mixing angles in the production moment t_0 and in a given moment t , and

$$\phi_m = \int_{t_0}^t dt' \Delta_m(t').$$

In the lowest order approximation for $\sin 2\theta_m$, $\sin 2\theta_m \approx \sin 2\theta\omega/V_e$, we find approximately:

$$P_{e\tau} = \frac{1}{4} \sin^2 2\theta\omega^2 \left[\frac{1}{V_e^2(t_0)} + \frac{1}{V_e^2(t)} - \frac{2}{V_e(t_0)V_e(t)} \cos \phi_m(t) \right]. \quad (68)$$

The background neutrinos are only subject to an electron background, so they will follow Eq. (68). The resonance value of the potential is $V_e^R = c_{2\theta}\omega_k$ and strong transformations occur when the final value of the potential $V_e(t) \ll V_e^R$, *i.e.* at very large distances.

In contrast, strong transformations of the probe neutrinos due to the parametric oscillations can occur at much smaller distances, determined by $V_\nu \gg c_{2\theta}\omega_k$. In the case of varying density, however, the conditions for parametric enhancement can be destroyed unless the density changes slowly enough.

For the probe neutrinos, the parametric resonance condition (48) can be satisfied in a certain layer of a medium with varying density. It can be rewritten as

$$\xi \approx A_\beta - 1. \quad (69)$$

So, it depends on the ratio of the potentials and essentially does not depend on the vacuum term. For a fixed A_β , Eq. (69) determines the resonance value ξ_R . The position of resonance is determined by $V_e \approx V_\nu/(A_\beta - 1)$ and it is much earlier (at higher densities) than the MSW resonance which occur at $V_e \approx c_{2\theta}\omega$. If the densities (potentials) change slowly enough, crossing the resonance can lead to strong flavor transformations.

We can generalise the usual MSW adiabatic condition to the case of parametric oscillations since the Hamiltonian (43) essentially coincides with the usual Hamiltonian. The difference is that the off-diagonal elements $\frac{1}{2}f' \approx s_{2\theta}\omega\xi$ (40) depend on the potential and that the diagonal elements depend on the densities giving a resonance at (69).

Let us compute the adiabaticity parameter in resonance which is given by the ratio of the spatial (evolution time) width of the resonance layer, Δt_R , and the oscillation length in the resonance l_m^R [33]:

$$\kappa_R = \frac{\Delta t_R}{l_m^R}. \quad (70)$$

Then, adiabaticity is satisfied if $\kappa_R > 1$.

Using Eq. (56), we obtain the width of resonance in the ξ , $\Delta\xi$:

$$\Delta\xi = \frac{f'}{V_e^R} = \frac{2s_{2\theta}\omega_k\xi}{V_e^R}. \quad (71)$$

Notice that in contrast to the width in energy, here the relative width is very small: $\Delta\xi/\xi \approx 10^{-3}$ for our benchmark values of parameters.

We assume that ξ has a power-law dependence on distance (evolution time)

$$\xi \propto t^\eta, \quad \dot{\xi} = \eta\xi/t_R,$$

where t_R determines the position of the resonance layer. Using this and Eq. (71) we find the spatial width of the resonance layer:

$$\Delta t_R = \frac{\Delta\xi}{\dot{\xi}} = \frac{2s_{2\theta}\omega_k t_R}{\eta V_e^R}. \quad (72)$$

Taking the position of the resonance layer to be $t_R \sim 0.5l_m^R$, we obtain

$$\kappa_R = \frac{s_{2\theta}\omega_k}{\eta V_e^R} \approx 3 \cdot 10^{-4}$$

by plugging Eq. (72) into Eq. (70). Thus, for the parameter values that we use and $\eta = \mathcal{O}(1)$, the adiabaticity is strongly broken. Adiabatic conversion would imply $\eta \approx 3 \cdot 10^{-4}$.

In this case one expects the following behaviour of the transition probability: Far from the parametric resonance layer, the adiabaticity is satisfied or weakly broken, so that $P_{e\tau}$ is parametrically enhanced in the way we discussed before. As the resonance (which is very narrow) is approached, the adiabaticity is broken and as it happens in the usual MSW case, $P_{e\tau}$ stops to increase and approaches some asymptotic value. In fact, κ_R gives an idea about the size of the asymptotic probability: $P_{e\tau}^{\text{ass}} \sim \kappa_R$.

The asymptotic value, $P_{e\tau}^{\text{ass}}$, can be estimated from the condition that in the spatial region Δt , where $P_{e\tau}^{\text{max}}$ (around the resonance) is bigger than $P_{e\tau}^{\text{ass}}$, one oscillation length is obtained:

$$\Delta t = l_m. \quad (73)$$

Here l_m is some effective value of the oscillation in the interval Δx . Recall that l_m is small at the edge of the interval but quickly increases towards the centre of the resonance. Using the expression for $P_{e\tau}^{\text{max}}$ in Eq. (55), we find that the region of ξ where $P_{e\tau}^{\text{max}} > P_{e\tau}^{\text{ass}}$ is given by

$$\Delta\xi_P = 2|\xi - \xi_R| = \frac{|f'|}{V_e^R \sqrt{P_{e\tau}^{\text{ass}}}}, \quad (74)$$

under the assumption that $P_{e\tau} \ll 1$. Then the corresponding spatial region equals

$$\Delta t = \frac{\Delta\xi_P}{\dot{\xi}} = \frac{\Delta\xi_P t}{\eta\xi}, \quad (75)$$

where again we assumed the power law for $\xi(t)$. The oscillation length at the border of the interval $\Delta\xi(t)$ is given by $2\pi/\gamma$. Since the interval is much bigger than the width of resonance, we can neglect f' in γ : $\gamma \approx |d - A_\beta \Delta_m| \approx V_e |\xi - \xi_R| = \frac{1}{2} V_e \Delta\xi_P$. Thus, the effective oscillation length equals

$$l_m = \frac{2\pi}{\gamma}, \quad (76)$$

Inserting (76) and (75) into our condition (73), we obtain

$$\frac{(\Delta\xi_P)^2 t}{\eta \xi} = \frac{4\pi}{V_e}.$$

Inserting here Eq. (74) for $\Delta\xi_P$ we obtain

$$P_{e\tau}^{\text{pass}} = \frac{f'^2 t}{4\pi\eta\xi V_e},$$

and finally, inserting $f' \approx 2s_{2\theta}\omega_p\xi$, we have

$$P_{e\tau}^{\text{pass}} = \frac{s_{2\theta}^2 \omega_p^2 \xi t_R}{\pi\eta V_e} = \frac{s_{2\theta}^2 \xi}{\pi\eta} \frac{\omega_p}{V_e} (\omega_p t_R). \quad (77)$$

For our benchmarks parameters and $\eta = 1$, we have from Eq. (77)

$$P_{e\tau}^{\text{pass}} = 3 \cdot 10^{-4}, \quad (78)$$

and the effective oscillation length in Eq. (76) is expected to be

$$l_m \omega_p \approx 4. \quad (79)$$

Furthermore, outside the resonance not only the gradient of ξ , but also the gradients of potentials separately determine the adiabaticity. Since the potentials have larger gradients, this suppresses the transition further.

6.2 Numerical solution

For illustration we take the background neutrino potential in the form

$$V_\nu^0 = \frac{6.5 \cdot 10^{10} \omega_p}{(t\omega_p + 10)^4}, \quad (80)$$

in our numerical computations, and for the potential due to scattering on electrons, we use two different profiles with high V_e^h and low V_e^l gradients:

$$V_e^h = \frac{10^{14} \omega_p}{(t\omega_p + 10)^5}, \quad V_e^l = \frac{1.8 \cdot 10^{12} \omega_p}{(t\omega_p + 10)^{4.2}}. \quad (81)$$

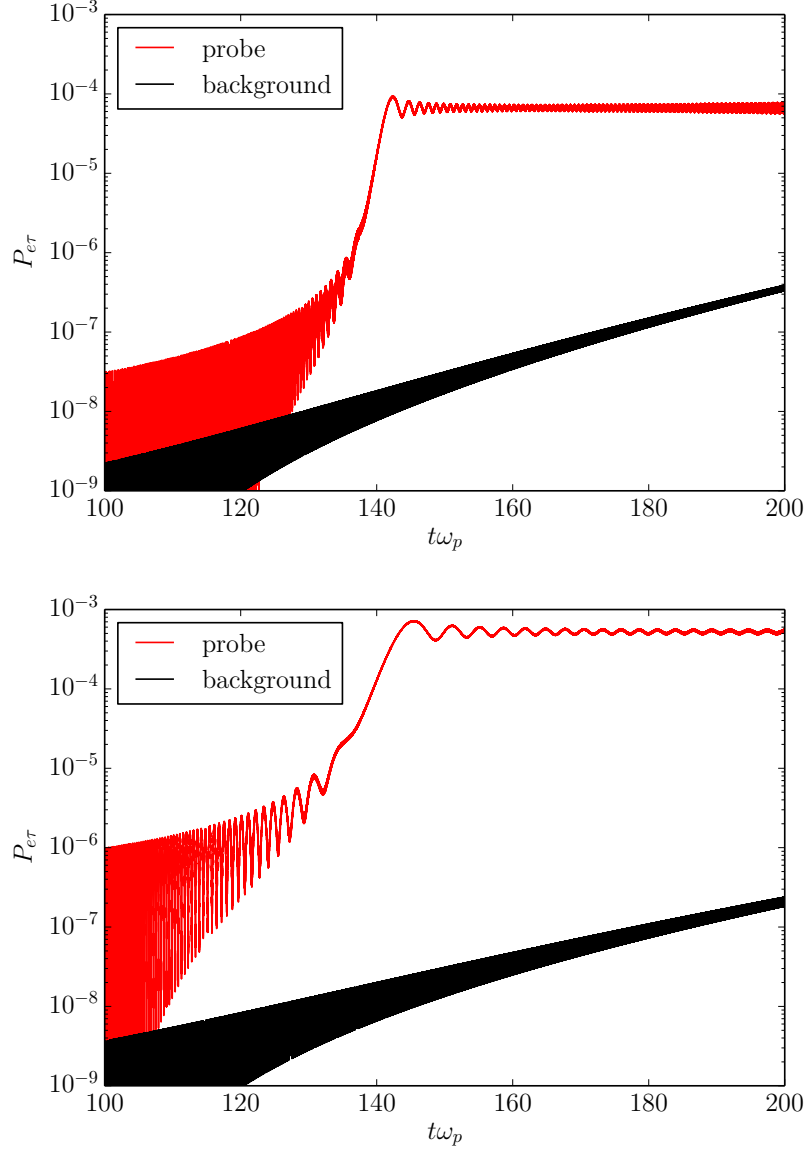


Figure 8: Conversion probability for changing densities. $\omega_k = \omega_p$ and $A_\beta = 1.0976$ such that the resonant condition is fulfilled at $t\omega_p = 140$. Upper panel: V_e^h (with high gradient), lower panel: V_e^h (with lower gradient).

These profiles are typical for a supernova during the accretion phase. The parameters in Eqs. (80) and (81) have been fixed in such a way that the benchmark values of $\xi \approx 0.1$, $V_e \approx 10^3 \omega_p$, and $V_\nu^0 \approx 10^2 \omega_p$ are achieved at $t\omega_p = 140$.

Using V_e , we first solved the evolution equation for the background neutrinos Eq. (19). Then, the obtained amplitudes ψ_e , ψ_τ and the probability $P_{e\tau}$ were used to solve the evolution equation for the probe neutrino. The results are shown in Figure 8. The evolution starts at $t\omega_p = 100$.

The lower black lines (areas) show the probabilities for the background neutrinos. Their average values follow the adiabatic solution in Eq. (68). For them the level crossing occur at $t\omega_p = 630$ (high gradient) and $t\omega_p = 830$ (low gradient) and the adiabaticity in the resonance is fulfilled in both cases. Notice that fast oscillations due to Δ_m are not resolved in the figures.

The upper (red) lines show the probabilities for the probe neutrinos. The oscillatory pattern of these lines is due to parametric oscillations. At $t\omega_p = 100$ the conversion probability of the probe neutrino is larger than that for the background neutrino due to parametric enhancement (although $\xi \ll \xi_R$). A zoom would reveal oscillations somewhat similar to the upper panel of Figure 4. Close to the parametric resonance at $t\omega_p = 140$, the conversion probability stops to increase and then approaches a constant value which is much smaller than 1. This is due to the breaking of adiabaticity as it was discussed in the previous section. The rapid rise takes place in $\Delta t\omega_p \sim 4$ in good agreement with Eq. (79) for $\eta = 1$, but the asymptotic value of P is smaller than the result in Eq. (78) by a factor of ~ 5 . This is due to the rapidly decreasing V_e and V_ν which has not been taken into account in Eq. (78).

With the decrease of the gradient η , the asymptotic value increases as $1/\eta$. For $\eta = 0.2$ that is a factor of ~ 5 which agrees well with the lower panel in Figure 8.

7 Conclusions

1. We develop an approach to the collective neutrino oscillations in supernova based on the flavor evolution of individual neutrinos in external potentials. The flavor evolution of supernovae neutrinos in the presence of the $\nu\nu$ interactions is linear in the sense that a given probe neutrino does not affect its own evolution as well as the evolution of other neutrinos which in turn could affect the probe neutrino. Therefore, the evolution is described by the usual Schrödinger-like equation with potentials generated by $\nu\nu$ scattering both in the diagonal and off-diagonal elements of the Hamiltonian. These potentials

have non-trivial dependence on the evolution time (distance) of the probe neutrino.

Consequently, an effective theory of collective oscillations based on certain assumptions on time dependence of the potentials can be developed. In particular, conditions for strong flavor transformations can be formulated. Strong transitions occur when the diagonal elements of the Hamiltonian vanish or when elements of the Hamiltonian have periodic time (distance) modulations. In the latter case, the parametric enhancement of flavor transitions can be realised.

2. To get an idea about the possible time dependence of the potentials, we considered a simplified solvable model of the background neutrinos which still retains the main feature of coherent flavor exchange. In this model a probe neutrino propagates in a flux of background neutrinos moving in the same direction so that $\nu\nu$ interactions in the flux are absent.

We have computed the potentials explicitly, and their main feature is the quasi-periodic dependence on time which is related to the flavor oscillations of the background neutrinos. The modulation frequency depends on V_e , V_ν and ω .

For certain conditions, periodic modulations of the potentials lead to parametric enhancement of the probe neutrino's oscillations. At the parametric resonance, the oscillations proceed with maximal depth. This indicates that, in the realistic case with $\nu\nu$ interactions in the flux, strong transitions can be interpreted as being due to a parametric resonance.

The relative width of the parametric resonance in the energy scale is proportional to the vacuum mixing and relative density of the background neutrinos $s_{2\theta}\xi$. The length of parametric oscillations in resonance is also given by $2\pi/(s_{2\theta}\xi\omega_p) = l_\nu/(s_{2\theta}\xi)$. So, with an increase of the neutrino density, the resonance becomes wider and the oscillation length smaller.

3. Integrations over the energy spectrum as well as over the production point of background neutrinos lead to strong suppression of the flavor transitions. Moreover, the latter is more important.

In the case of varying densities, and consequently potentials, strong transitions are possible if the adiabaticity condition is satisfied in the parametric resonance. We find that the adiabaticity is strongly broken for typical parameters of supernovae, thus leading to strong suppression of flavor transformations.

Integration over the angles in the background would imply $\nu\nu$ interactions and so can not be described without changing the dynamics of the model. One exception is when the background neutrino flux is emitted from a small

sphere, such that there is no $\nu\nu$ interactions in the flux, but a probe neutrino will see background neutrinos with changing angle or A_β . The effect is similar to the case of a varying neutrino density.

4. The main question is to which extend our conclusions for the simplified model of the background can be extended to the realistic case with $\nu\nu$ interactions in the flux. Our results imply that extremely strong correlations (tuning) between the evolution of the probe and background neutrinos is required in order to get strong transitions. Turning on the $\nu\nu$ interactions in the background can in general lead to an enhancement of transitions in the background (instead of constant $P_{e\tau}^{\max}$), and consequently to faster transitions of the probe neutrino. At this point one can use iteration: Take the solution found for the probe neutrino due to parametric enhancement and use it as the background for the flux neutrinos.

The $\nu\nu$ interactions in the background can lead to a larger correlation between the background and probe neutrinos. An increase of ξ can lead to an extension of the region of strong effects in energy scale and to some extent mitigate the averaging over energy. It also improves adiabaticity. A detailed study with iterations will be presented elsewhere [34].

Acknowledgements

R.S.L.H. is funded by the Alexander von Humboldt Foundation. The work of A.S. is supported by Max-Planck senior fellow grant M.FW.A.KERN0001.

Appendix A. No neutrino background effect for $A_\beta = 1$

For $A_\beta = 1$ the flavor evolutions of the probe neutrino and the neutrino from the flux are identical. This can be understood considering collisions of the probe neutrino with individual neutrinos from the flux. In each collision (starting from the first one) flavor exchange does not produce any change. Both neutrinos (probe and flux) arrive at the collision point (point of crossing of trajectories) in the same state. Therefore the flavor exchange does not produce any change. As a result, the effect of neutrino-neutrino interactions drops out. In our formalism this is obtained since the neutrino state becomes the eigenstate of the part of the Hamiltonian which depends on the neutrino

densities. Indeed, according to (2)

$$H_\nu \psi = V_\nu^0 \begin{pmatrix} \psi_e \psi_e^* & \psi_e \psi_\tau^* \\ \psi_e^* \psi_\tau & \psi_\tau \psi_\tau^* \end{pmatrix} \begin{pmatrix} \psi_e \\ \psi_\tau \end{pmatrix} = V_\nu^0 \begin{pmatrix} \psi_e \\ \psi_\tau \end{pmatrix},$$

where we added the matrix $0.5(\psi_e \psi_e^* + \psi_\tau \psi_\tau^*)I$ proportional to the unit matrix (which does not affect flavor evolution), and we have taken into account that $\psi_e \psi_e^* + \psi_\tau \psi_\tau^* = 1$. Thus $H_\nu \psi = V_\nu^0 I \psi$, that is the contribution to the Hamiltonian from neutrino - neutrino interactions is proportional to the unit matrix and therefore can be omitted.

Appendix B. Correction due to the non-resonant mode

Let us search for a solution of the evolution equation with the complete Hamiltonian (42) in the form

$$S_\alpha = S_0 S_1, \quad (82)$$

where S_0 is given in (46). Inserting S_α in the evolution equation with the total Hamiltonian and taking into account (45), we obtain the equation for S_1 :

$$i\dot{S}_1 = \Delta H_1 S_1, \quad \Delta H_1 \equiv S_0^\dagger \Delta H^\alpha S_0.$$

Let us find the solution of this equation in the resonance: $A_\beta \Delta_m = d$, (48) when $\theta_m^p = \pi/4$. In this case the matrix (46) simplifies

$$S_0 = \begin{pmatrix} \cos \phi_m^p & -i \sin \phi_m^p \\ -i \sin \phi_m^p & \cos \phi_m^p \end{pmatrix}. \quad (83)$$

Then the Hamiltonian ΔH_1 in (46) becomes

$$\Delta H_1 = \frac{f'}{4} \begin{pmatrix} \sin 2\phi_m^p \sin 2\phi_m & \cos 2\phi_m + i \cos 2\phi_m^p \sin 2\phi_m \\ \cos 2\phi_m - i \cos 2\phi_m^p \sin 2\phi_m & -\sin 2\phi_m^p \sin 2\phi_m \end{pmatrix}.$$

Here $2\phi_m^p = \gamma t = \frac{1}{2}f't$. In Eq. (83) we have two frequencies $\frac{1}{2}f' \ll 2A_\beta \Delta_m \propto 2V_e$. It is this large frequency $A_\beta \Delta_m$ that modulates the oscillations generated by (83).

The off-diagonal element of (83) can be written as

$$(\Delta H_1)_{12} = z e^{i\chi},$$

where

$$z \equiv \sqrt{1 - \eta^2}, \quad \sin \chi = \frac{1}{z} \sin 2\phi_m \cos 2\phi_m^p \quad (84)$$

and

$$\eta \equiv \sin 2\phi_m \sin 2\phi_m^p.$$

In terms of η and χ the Hamiltonian can be rewritten as

$$\Delta H_1 = \frac{f'}{4} \begin{pmatrix} \frac{\eta}{\sqrt{1 - \eta^2} e^{-i\chi}} & \sqrt{1 - \eta^2} e^{i\chi} \\ \sqrt{1 - \eta^2} e^{-i\chi} & -\eta \end{pmatrix}. \quad (85)$$

Let us make a transformation of the fields

$$\psi_\alpha = U_\chi \psi_\chi, \quad U_\chi = \text{diag} \left(e^{i\frac{\chi}{2}}, e^{-i\frac{\chi}{2}} \right)$$

that eliminates the phase from the off-diagonal elements of (85). Then the evolution equation of the transformed fields, ψ_χ , has the Hamiltonian

$$\Delta H_\chi = -\frac{1}{2} \begin{pmatrix} \frac{1}{2} f' \eta + \dot{\chi} & \frac{1}{2} f' \sqrt{1 - \eta^2} \\ \frac{1}{2} f' \sqrt{1 - \eta^2} & -\frac{1}{2} f' \eta - \dot{\chi} \end{pmatrix}. \quad (86)$$

Since $A_\beta \Delta_m \gg f$ at early times of evolution, we can take $\sin 2\phi_m^p \approx 0$, and consequently, $\eta \approx 0$. In this case the Hamiltonian (86) becomes

$$\Delta H_\chi = \frac{1}{2} \begin{pmatrix} \dot{\chi} & \frac{f'}{2} \\ \frac{f'}{2} & -\dot{\chi} \end{pmatrix}.$$

According to (84) $\chi \approx 2\phi_m$, so that $\dot{\chi} \approx 2A_\beta \Delta_m$. Therefore ΔH_χ describes oscillations with large frequency (total level split):

$$\sqrt{\dot{\chi}^2 + (f'/2)^2} \approx \dot{\chi}$$

and with the depths

$$\sin^2 2\theta_\chi = \frac{f'^2}{4\dot{\chi}^2 + f'^2} \approx \frac{f'^2}{4\dot{\chi}^2} \approx \frac{f'^2}{16A_\beta^2 \Delta_m^2}.$$

The corresponding S_χ matrix has the same form as in (46) with $\theta_m^p \rightarrow \theta_\chi$ and

$$\phi_m^p \rightarrow \phi_\chi = \frac{1}{2} t \sqrt{\dot{\chi}^2 + (f'/2)^2} \approx \frac{1}{2} t \dot{\chi} = \frac{1}{2} \chi.$$

In the first approximation in small mixing θ_χ , we have

$$S_\chi \approx \begin{pmatrix} e^{i\phi_\chi} & -i \sin 2\theta_\chi \sin \phi_\chi \\ -i \sin 2\theta_\chi \sin \phi_\chi & e^{-i\phi_\chi} \end{pmatrix}.$$

Returning back to the α basis gives

$$S_1 = U_\chi S_\chi U_\chi^\dagger \approx \begin{pmatrix} e^{i\phi_\chi} & -i\epsilon e^{i\chi} \\ -i\epsilon e^{-i\chi} & e^{-i\phi_\chi} \end{pmatrix}, \quad (87)$$

where $\epsilon \equiv \sin 2\theta_\chi \sin \phi_\chi$. The total S matrix equals the product (82) of S_0 in (83) and S_1 (87):

$$S_0 S_1 = \begin{pmatrix} \cos \phi_m^p e^{i\phi_\chi} - \epsilon \sin \phi_m^p e^{-i\chi} & -i(\sin \phi_m^p e^{-i\phi_\chi} + \epsilon \cos \phi_m^p e^{i\chi}) \\ -i(\sin \phi_m^p e^{i\phi_\chi} + \epsilon \cos \phi_m^p e^{-i\chi}) & \cos \phi_m^p e^{-i\phi_\chi} - \epsilon \sin \phi_m^p e^{i\chi} \end{pmatrix}.$$

Rotating back to the flavor basis

$$S = U U_\alpha S_0 S_1 U_\alpha^\dagger U^\dagger,$$

we obtain for the 12 element:

$$S_{12} = \sin \phi_m^p e^{-i(\phi_\chi + \phi_m)} + \cos \phi_m^p \sin \phi_\chi \left(\sin 2\theta_\chi e^{i(\chi - \phi_m)} - \frac{g}{d} \right),$$

where a common factor $-i$ is omitted. Then keeping the first correction to the main (first) term, we have for the probability

$$P_{e\tau}^p \approx \sin^2 \phi_m^p + \sin 2\phi_m^p \sin \phi_m \left[\sin 2\theta_\chi \cos 3\phi_m - \frac{g}{d} \cos 2\phi_m \right], \quad (88)$$

where we used that $\phi_\chi \approx \frac{1}{2}\chi \approx \frac{1}{2}\phi_m$.

Thus, the zero order solution given by the first term $\sin^2 \phi_m^p$ (oscillations with maximal depth and large period given by f' in our example) is modulated by fast oscillations ($2A_\beta \Delta_m$ frequency) with small depth proportional to

$$\sin 2\theta_\chi \sim \frac{f'}{\dot{\chi}} \sim \frac{f'}{A_\beta \Delta_m} \sim \frac{s_{2\theta} \omega_k \xi}{V_e} \quad \text{and} \quad \frac{g}{d} \sim \frac{s_{2\theta} \omega_k}{V_e}.$$

Let us compare the probability in (88) which takes into account corrections due to the non-resonant mode ($S_1(\Delta H^\alpha)$ and corresponds to the exact resonance, and the lowest order (S_0) probability in Eq. (47) which can be used also outside the resonance. We can rewrite Eq. (88) as

$$P_{e\tau}^p \approx \left[1 - \frac{g}{d} \frac{1}{\tan \frac{1}{2}\gamma t} \sin \phi_m \left(\cos 2\phi_m - \frac{f'}{4g} \cos 3\phi_m \right) \right] \sin^2 \frac{1}{2}\gamma t. \quad (89)$$

In turn, the probability (47) equals approximately

$$P_{e\tau}^p = \frac{1}{\gamma^2} \left[\frac{f'^2}{4} + \frac{g}{d} (d - A_\beta \Delta_m) f' \cos \phi_m \right] \sin^2 \frac{1}{2}\gamma t.$$

In resonance $P_{e\tau}^p = \sin^2 \frac{1}{2} \gamma t$. Close to resonance, $|d - A_\beta \Delta_m| \sim |f'|$, we have

$$P_{e\tau}^p \approx \frac{f'^2}{4\gamma^2} \left(1 + \frac{4g}{d} \cos \phi_m \right) \sin^2 \frac{1}{2} \gamma t.$$

The coefficient in front of $\cos \phi_m$ has smallness $\sim \frac{g}{d}$ with respect to the first term. Comparing this with (89), we conclude that the oscillating term that arises from the transformation from S_α to S is comparable to the correction that arises from S_1 (88). In resonance, modulations due to transition to the α basis are absent and the modulations are due to the S_1 correction only. According to (89) corrections to the probability due to S_1 can be enhanced due to $\tan \frac{1}{2} \gamma t$ in the early evolution when the phase is small.

Hence Eq. (47) is not correct to order $\frac{g}{d}$. However, for the hierarchy $V_e \gg V_\nu \gg \omega$, the correction $\frac{g}{d} \ll \xi$ and the analytic approximation is still valid.

References

- [1] J. T. Pantaleone, Phys. Lett. B **287** (1992) 128. doi:10.1016/0370-2693(92)91887-F
- [2] H. Duan, G. M. Fuller and Y. Z. Qian, Phys. Rev. D **74** (2006) 123004 doi:10.1103/PhysRevD.74.123004 [astro-ph/0511275].
- [3] H. Duan, G. M. Fuller, J. Carlson and Y. Z. Qian, Phys. Rev. D **74** (2006) 105014 doi:10.1103/PhysRevD.74.105014 [astro-ph/0606616].
- [4] H. Duan, G. M. Fuller, J. Carlson and Y. Z. Qian, Phys. Rev. Lett. **97** (2006) 241101 doi:10.1103/PhysRevLett.97.241101 [astro-ph/0608050].
- [5] S. Hannestad, G. G. Raffelt, G. Sigl and Y. Y. Y. Wong, Phys. Rev. D **74** (2006) 105010 Erratum: [Phys. Rev. D **76** (2007) 029901] doi:10.1103/PhysRevD.74.105010, 10.1103/PhysRevD.76.029901 [astro-ph/0608695].
- [6] G. L. Fogli, E. Lisi, A. Marrone and A. Mirizzi, JCAP **0712** (2007) 010 doi:10.1088/1475-7516/2007/12/010 [arXiv:0707.1998 [hep-ph]].
- [7] G. G. Raffelt and A. Y. Smirnov, Phys. Rev. D **76** (2007) 081301 Erratum: [Phys. Rev. D **77** (2008) 029903] doi:10.1103/PhysRevD.76.081301, 10.1103/PhysRevD.77.029903 [arXiv:0705.1830 [hep-ph]].

- [8] G. G. Raffelt and A. Y. Smirnov, Phys. Rev. D **76** (2007) 125008 doi:10.1103/PhysRevD.76.125008 [arXiv:0709.4641 [hep-ph]].
- [9] B. Dasgupta, A. Dighe, G. G. Raffelt and A. Y. Smirnov, Phys. Rev. Lett. **103** (2009) 051105 doi:10.1103/PhysRevLett.103.051105 [arXiv:0904.3542 [hep-ph]].
- [10] B. Dasgupta, A. Dighe, A. Mirizzi and G. G. Raffelt, Phys. Rev. D **77** (2008) 113007 doi:10.1103/PhysRevD.77.113007 [arXiv:0801.1660 [hep-ph]].
- [11] S. Chakraborty, R. S. Hansen, I. Izaguirre and G. Raffelt, JCAP **1603** (2016) no.03, 042 doi:10.1088/1475-7516/2016/03/042 [arXiv:1602.00698 [hep-ph]].
- [12] R. F. Sawyer, Phys. Rev. D **79** (2009) 105003 doi:10.1103/PhysRevD.79.105003 [arXiv:0803.4319 [astro-ph]].
- [13] R. F. Sawyer, Phys. Rev. D **72** (2005) 045003 doi:10.1103/PhysRevD.72.045003 [hep-ph/0503013].
- [14] B. Dasgupta, A. Mirizzi and M. Sen, JCAP **1702** (2017) no.02, 019 doi:10.1088/1475-7516/2017/02/019 [arXiv:1609.00528 [hep-ph]].
- [15] B. Dasgupta and M. Sen, arXiv:1709.08671 [hep-ph].
- [16] I. Izaguirre, G. Raffelt and I. Tamborra, Phys. Rev. Lett. **118** (2017) no.2, 021101 doi:10.1103/PhysRevLett.118.021101 [arXiv:1610.01612 [hep-ph]].
- [17] F. Capozzi, B. Dasgupta, E. Lisi, A. Marrone and A. Mirizzi, Phys. Rev. D **96** (2017) no.4, 043016 doi:10.1103/PhysRevD.96.043016 [arXiv:1706.03360 [hep-ph]].
- [18] S. Abbar and H. Duan, arXiv:1712.07013 [hep-ph].
- [19] A. Esteban-Pretel, A. Mirizzi, S. Pastor, R. Tomas, G. G. Raffelt, P. D. Serpico and G. Sigl, Phys. Rev. D **78** (2008) 085012 doi:10.1103/PhysRevD.78.085012 [arXiv:0807.0659 [astro-ph]].
- [20] S. Chakraborty, R. S. Hansen, I. Izaguirre and G. Raffelt, JCAP **1601** (2016) no.01, 028 doi:10.1088/1475-7516/2016/01/028 [arXiv:1507.07569 [hep-ph]].

- [21] B. Dasgupta and A. Mirizzi, Phys. Rev. D **92** (2015) no.12, 125030 doi:10.1103/PhysRevD.92.125030 [arXiv:1509.03171 [hep-ph]].
- [22] F. Capozzi, B. Dasgupta and A. Mirizzi, JCAP **1604** (2016) no.04, 043 doi:10.1088/1475-7516/2016/04/043 [arXiv:1603.03288 [hep-ph]].
- [23] R. S. Hansen and S. Hannestad, Phys. Rev. D **90** (2014) no.2, 025009 doi:10.1103/PhysRevD.90.025009 [arXiv:1404.3833 [hep-ph]].
- [24] G. Mangano, A. Mirizzi and N. Saviano, Phys. Rev. D **89** (2014) no.7, 073017 doi:10.1103/PhysRevD.89.073017 [arXiv:1403.1892 [hep-ph]].
[25]
- [25] G. Raffelt, S. Sarikas and D. de Sousa Seixas, Phys. Rev. Lett. **111** (2013) no.9, 091101 Erratum: [Phys. Rev. Lett. **113** (2014) no.23, 239903] doi:10.1103/PhysRevLett.113.239903, 10.1103/PhysRevLett.111.091101 [arXiv:1305.7140 [hep-ph]].
- [26] G. D. Pusch, Nuovo Cim. A **74** (1983) 149. doi:10.1007/BF02902503
- [27] V. K. Ermilova, V. A. Tsarev, and V. A. Chechin, Kratk. Soobshch. Fiz. **5** 26 (1986)
- [28] E. K. Akhmedov, Sov. J. Nucl. Phys. **47** (1988) 301 [Yad. Fiz. **47** (1988) 475].
- [29] P. I. Krastev and A. Y. Smirnov, Phys. Lett. B **226** (1989) 341. doi:10.1016/0370-2693(89)91206-9
- [30] E. K. Akhmedov, Nucl. Phys. B **538** (1999) 25 doi:10.1016/S0550-3213(98)00723-8 [hep-ph/9805272].
- [31] I. Tamborra, L. Huedepohl, G. Raffelt and H. T. Janka, Astrophys. J. **839** (2017) 132 doi:10.3847/1538-4357/aa6a18 [arXiv:1702.00060 [astro-ph.HE]].
- [32] M. T. Keil, G. G. Raffelt and H. T. Janka, Astrophys. J. **590** (2003) 971 doi:10.1086/375130 [astro-ph/0208035].
- [33] S. P. Mikheev and A. Y. Smirnov, Nuovo Cim. C **9** (1986) 17. doi:10.1007/BF02508049
- [34] R. S.L. Hansen, A. Y. Smirnov, work in progress.